INVESTIGATION OF THE STATISTICS OF PURE TONE SOUND POWER INJECTION FROM LOW FREQUENCY, FINITE SIZED SOURCES IN A REVERBERANT ROOM

BY

WAYNE FARRIOR SMITH

CENTER FOR ACOUSTICAL STUDIES
DEPARTMENT OF MECHANICAL AND AEROSPACE ENGINEERING
NORTH CAROLINA STATE UNIVERSITY
RALEIGH, NORTH CAROLINA

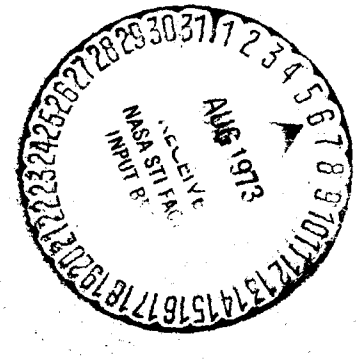

MAY 1973

ABSTRACT

SMITH, WAYNE FARRIOR. Investigation of the Statistics of Pure Tone Sound Power Injection from Low Frequency, Finite Sized Sources in a Reverberant Room. (Under the direction of JAMES RONALD BAILEY and FRANKLIN DELANO HART).

The measurement of sound power injection into a reverberant room is subject to statistical uncertainties owing to large fluctuations of sound pressure level with variations in source frequency and source and/or receiver position. Especially with regard to low frequency pure tone sources, point source theory indicates a requirement of many microphone and source positions if radiated power is to be accurately measured.

An investigation has been conducted to determine the effect of finite source size on the power statistics in a reverberant room for pure tone excitation. Theoretical results indicate that the standard deviation of low frequency, pure tone finite sources is always less than that predicted by point source theory and considerably less when the source dimension approaches one-half an acoustic wavelength or greater.

A supporting experimental study was conducted utilizing an eight inch loudspeaker and a 30 inch loudspeaker at eleven source positions. The resulting standard deviation of sound power output of the smaller speaker is in excellent agreement with both the derived finite source theory and existing point source theory, if the theoretical data is adjusted to account for experimental incomplete spatial averaging. However, the standard deviation of sound power output of the larger speaker is measurably lower than point source theory indicates, but is in good agreement with the finite source theory developed in this work.

BIOGRAPHY

Wayne F. Smith was born [redacted] in [redacted]. He received his elementary and secondary education in Greensboro and graduated from Grimsley High School in 1965.

He entered North Carolina State University in 1965 majoring in mechanical engineering. During the summers while an undergraduate, he served as an engineer trainee for National Aeronautics and Space Administration at Langley Research Center and as a research assistant in studies sponsored by Shell Oil Company and the National Science Foundation. He received his Bachelor of Science degree in the honors program in 1969.

Since 1969, he has dedicated full time to graduate study within the Center for Acoustical Studies, a special organization in the Department of Mechanical and Aerospace Engineering at North Carolina State University. His studies have included both the teaching of undergraduate courses in mechanical engineering and the performing of consulting services in acoustics.

The author is married to the former Miss Arlyss Susan Caudle, and they have one daughter - Kimberly Ann.

ACKNOWLEDGMENTS

The author wishes to express his gratitude to his Committee Co-chairmen, Dr. J. R. Bailey and Dr. F. D. Hart, for their help in suggesting the topics investigated in this thesis. Special thanks are expressed to Dr. Bailey, whose guidance, encouragement, and assistance throughout the course of the research, enabled the realization of the final goals. Appreciation is also extended to the other committee members, including Dr. L. H. Royster, Dr. J. C. Williams, and Dr. M. H. Clayton. Professor A. H. Grandage also made helpful suggestions on statistical problems.

Much of the financial burden of this research study was alleviated by financial assistance through an acoustics traineeship program sponsored by the National Aeronautics and Space Administration, NGL -34-002-035

Finally, the author expresses his thanks to his wife, Candy, for her patience and encouragement, and for the many sacrifices which both she and their daughter, Kimberly, have been required to make during this period.

TABLE OF CONTENTS

LIST OF TABLES

LIST OF FIGURES

LIST OF FIGURES (continued)

1. INTRODUCTION

Noise has long been recognized as a cause of annoyance and physiological damage to the human body. Before 1960, sporatic attempts were made to study and reduce this noise pollution problem, but no overall trend in this direction was manifest. However, recent public pressure and interest in noise has prompted considerable noise reduction research and legislative action. This new found interest in conquering the noise problem is exemplified by a special awareness toward the elimination of occupational deafness due to intense noise exposure. The Williams-Steiger Occupational Safety and Health Act of 1970 (25) has established a list of noise criteria which must be met by industries engaged in interstate commerce. The industries involved must comply with the established requirements or be subject to severe economic repercussions.

One important compliance criterion of the Occupational Safety and Health Act (OSHA) involves the initiation of an engineering program to study and to reduce sound levels at their sources. This engineering study would, of course, include either retrofitting or redesign of existing noisy machinery or the purchase of new machinery designed to meet compliance standards. In either case, the ultimate objective would be to reduce the sound pressure level within the industrial environment at locations occupied by working personnel. Several industries have been designated as target areas in the enforcement of the OSHA. These include longshoremen, roofing and sheet metal, meat products, mobile home manufacturing, and lumber and wood products.

The potential economic impact upon these industries of the strict enforcement of this act cannot be overemphasized.

But the problems associated with any program designed to reduce noise levels involves the ability to evaluate accurately the acoustic benefit of retrofit and redesign or the ability to purchase new equipment with confidence that noise levels in the acoustic environment will truly be improved. Modifications made to existing machinery mounted in its normal operating position in the acoustic environment presents little, if any, problem. Comparative sound level measurements taken at normal personnel locations will indicate any beneficial changes. However, for any redesign done remote from the actual machine location or with regard to prospective machine purchases, sound pressure level alone is not a satisfactory measure of noise source strength. This is due to the fact that sound pressure level varies with the distance between the source and receiver and with the environment for both. The acoustic power and directivity of a source are the fundamental quantities needed to describe acoustic performance.

The acoustic power of a sound source is a measure of the total energy per unit time radiated in all directions, stated as a function of frequency. The acoustic directivity of a source is a measure of the change in power radiation magnitude with changes in angular position, also stated as a function of source frequency. Given the acoustic power and directivity, it is possible to make an engineering estimate of the resultant sound pressure levels generated by a source in almost any acoustic environment. Moreover, the acoustic power is often used by itself to compare the acoustic merits of different source designs.

In addition to the obvious beneficial application to machinery noise reduction research, acoustic power measurements could also play a big part in the establishment of product noise codes in the near future. It is anticipated that, due to annoyance considerations, such products as household appliances, lawnmowers, air conditioners, and motor vehicles will be required to meet noise emission standards. Sound power measurements could play a significant role in the establishment of such noise standards. Thus, the need to understand and to develop an accurate and economical method of determining the sound power output of any given source is quite evident.

In order to measure sound power with a high degree of confidence, special acoustical environments are required. One type of environment which is acceptable is termed anechoic. An anechoic facility is constructed by treating all the bounding surfaces of a room with sound absorbing wedges so that approximately 99 percent of the incident acoustic energy is absorbed within a typical frequency range from 150 Hz to 10,000 Hz. The source under test is usually placed on a suspended floor within the facility and measurements of sound pressure level are made at specific locations on an imaginary hemisphere surrounding the source. Due to the free field environment existing in such a room, the sound level measurements enable one to accurately determine the free field sound power output of the source, in addition to its directivity characteristics. Such directivity is extremely important in the prediction of the noise level at any given location in an actual industrial environment. Obviously, the complete and accurate description of the sound power characteristics of a complicated source in an anechoic facility generally requires the

assimilation of a considerable quantity of data. Thus, in terms of man-hours, the test effort involved is relatively high. Additionally, the design and construction of an anechoic chamber requires a relatively high monetary investment. As a result, only a few anechoic facilities are in existence in the United States and these are by no means readily available for the volume of sound power measurements anticipated in the near future.

The converse of the anechoic environment is the reverberant environment. A reverberation chamber is designed so that the bounding surfaces absorb very little acoustic energy, resulting in a highly reflective, diffuse sound field. Generally speaking, sound power measurements in a diffuse sound field require less test effort due to the fewer number of microphone readings and the less accurate microphone placement required. For sources radiating essentially broad band noise, the diffuse field sound reflections average out in the room and the average of only a few microphone readings is well representative of the spatial average pressure in the room. Sources which exhibit strong pure tones or narrow bands of noise, however, can generate standing waves, thereby resulting in large fluctuations in sound pressure with variations in source frequency as well as source and/or receiver positions. Associated with these fluctuations and variations is a certain amount of statistical uncertainty which must be fully understood in detail before pure tone measurements can be undertaken with confidence. Thus, the reverberation room technique, which was first thought to be an effective tool for acoustic research, has

developed into a research obstacle which must first be understood before it can be effectively used for pure tone measurement.

The state-of-the-art for reverberant rooms is fairly well established for broad-band, narrow-band, and pure tone excitations if the source is assumed to exhibit monopole type radiation characteristics and to be located at a point in the reverberant field. However, the majority of real sources are not located at a point but are distributed over some finite area. Therefore, this study is designed to investigate the effects of finite source size on the low frequency variance of acoustic power for a monopole type pure tone source in a reverberant room. The theory developed would be equally applicable to high frequency variance; but, as pointed out by Baade[1], the total variance at high frequency is relatively small so that any change due to finite source size would be of little practical importance.

The presentation of this study begins in Chapter 2 with a review of the present state of the art in reverberant room power measurements. In this literature review, special emphasis is placed on reverberant rooms excited by pure tone sources.

In Chapter 3, the output power statistics for a pure tone point source are reviewed. This theory is then extended in Chapter 4 to include finite source dimensions. The analysis of the finite source model is discussed in detail with the results expressed in terms of corresponding point source theory.

---

[1]This remark was made to the Acoustical Society of America as part of the introduction and discussion for the Symposium on Sound Power Measurements in Reverberant Rooms, November 22, 1968.

Chapter 5 provides a complete description of the reverberation facility which was utilized in obtaining experimental results in support of the theoretical derivations. This description includes both theoretical and experimental calculations of room acoustic properties, as well as a thorough description of the experimental setup. Special emphasis is placed on a description of the microphone traversing apparatus which was specially designed and constructed for use in this study. Finally, the statistical analysis of the data utilizing a two way analysis of variance is discussed in detail and the corresponding results are presented.

In Chapter 6, the experimental results are compared to both point source theory and the derived finite source theory. Special emphasis is placed upon the necessary adjustment of the theoretical results to account for the experimentally incomplete spatial averaging.

Finally, in Chapter 7, the significant findings and contributions of this study are summarized and conclusions are drawn. These conclusions include suggestions for expanding this study, as well as a brief discussion of some other problems, yet unsolved, associated with reverberant rooms.

2. REVIEW OF THE LITERATURE

The study of reverberation environments and the properties of such environments which made them suitable for acoustic power measurements is only a small part of a larger area of research known as room acoustics. Although the acoustics of enclosed spaces has been of obvious importance since the first auditoriums and theaters were built, it was late in the nineteenth century before the maze of superstition surrounding the subject began to be replaced by scientific explanation. But major breakthroughs were still slow in coming; in fact, it was not until the last two decades that a basic understanding of reverberant field power measurements began to be developed.

The first major development concerning the acoustic properties of large enclosures was made by Sabine (19) in 1895. Through extensive experimental studies, Sabine arrived at a mathematical relationship between the reverberation characteristics of an enclosure, its volume, and the amount of absorption present. This relationship is given by

$$T = \frac{0.049V}{S\bar{\alpha}} \quad , \tag{2.1}$$

where T is the reverberation time of the enclosure in seconds, V is the room volume in cubic feet, S is the room surface area in square feet, and $\bar{\alpha}$ is the average absorption coefficient of the room. His definition of reverberation time as the time in seconds required for a 60 dB decrease in sound intensity is still the single, most important parameter in judging the quality of an acoustic environment. Theoretical derivations of (2.1) are usually based on geometric acoustics in which

sound is assumed to travel in rays (17). At each encounter with a boundary, the rays are partially absorbed and partially reflected. Although this theory often oversimplifies the actual behavior of waves in rooms, it leads to valid results under certain specific conditions. If the absorptive capability of the room is high, the number of wall reflections is small, the reverberation time is small, and the ultimate sound intensity at any point is quickly reached. Such rooms deviate greatly from Sabine's theory. On the other hand, if the absorption is low, the intensity growth rate is small and the reverberation time is large. Rooms of this type are known as live or reverberation rooms, and application of Sabine's theory produces accurate results.

For sound sources started in a live room such as described above, many reflections at the walls produce a sound energy distribution that becomes more and more uniform with time (16). Ultimately, this energy density may be assumed to be uniform, with completely random directions of flow. Such a condition, known as diffuse, is extremely important in room acoustics due to its relative ease of description using normal mode and statistical techniques.

Large rooms under diffuse conditions can be used to accurately measure the absorption and transmission loss of acoustical materials and the sound power output of acoustical sources. The problem, however, which arose early in reverberation room research, and a problem which still exists to some extent today, is the establishment of a valid criterion to determine whether the sound field in an enclosure can be assumed to be diffuse (21). A large reverberation time would tend to

indicate diffuse conditions, but the intimate relationship among room volume, excitation frequency, and the amount and location of absorption prevents the establishment of any limiting value for an acceptable reverberation time.

The simplest method to date for determining the existence of diffuse conditions involves the calculation of Schroeder's "large room frequency" (20), given by

$$f_s = 1.19 \times 10^4 \left(\frac{T}{V}\right)^{1/2} , \qquad (2.2)$$

where T and V are as defined for (2.1). This quantity describes the low frequency cutoff above which the sound in a particular room may be approximated as diffuse. Experimental results, however, have shown this number to be quite conservative, in that data taken one octave or more lower has exhibited satisfactory diffuse characteristics (7).

To help alleviate the obvious problems which exist concerning the diffuse field approximation, ASHRAE Standard 36-62 is often utilized (1,22). But this qualification procedure lacks consideration of recent developments and is, consequently, rather incomplete as far as pure tone testing is concerned. An improved test procedure, therefore, is presently under draft which hopefully will define completely both the usable frequency range of any reverberation facility and the test procedure for pure tone and narrow-band testing.

With the importance of diffusiveness firmly established, several other parameters and their effect on reverberant room power measurements need to be discussed. A number of studies (6, 7, 12, 14, 20, 26) have been carried out on the fluctuations in room sound pressure when the

frequency of the source is varied or when the position of the source or receiver is varied. These fluctuations give rise to statistical uncertainties which must be resolved and understood before accurate measurements can be performed. For broad-band noise, theory and experiment indicate very little uncertainty, except in cases of very low room absorption (2). This is because the spatial fluctuation of pressure throughout the room is small and the change in the reaction of the room environment on the source is quite small. However, problems arise in trying to measure the sound power of sources exhibiting discrete frequencies. Much of the current research in room acoustics has been aimed at understanding and solving the problems of pure tone measurements.

The statistics of source irregularity (frequency irregularity), originally studied by Bolt and Roop (6), was revised and extended by Schroeder (20). He found that if the large room frequency was satisfied, the standard deviation from the mean of room sound pressure level due to changes in source frequency was 5.57 dB. Furthermore, it was found that the lesser the degree of room symmetry, the greater was the degree of sound diffusiveness. The room irregularities decrease the concentrated areas of degenerate modes in the room frequency response.

In 1959, Doak (7) investigated the fluctuations in sound pressure level when the receiver position is varied - space irregularity. Using both theoretical and experimental techniques, the standard deviation of sound pressure level from its mean for a pure tone source was found to be the same for variations in receiver position as it is for variations in source frequency, namely 5.57 dB. This value, however, is only valid for receiver positions far from the source and beyond one-quarter of a

wavelength from the room walls and for frequencies near or above the large room frequency.

In several later publications, Lubman expanded upon Doak's work to better describe the fluctuations in pure tone pressure due to receiver position. In 1968 (12), he showed that the standard deviation of pure tone pressure normalized to the mean has a value of unity. This was followed in 1969 (13) by a discussion of the reduction in normalized standard deviation by a ratio of $\sqrt{N}$ if N independent samples of the sound field are averaged. These independent samples can either be taken discretely at half-wavelength intervals or be obtained by averaging over a straight line traverse. The equivalent number of independent samples in a traverse is given by $N = 1 + 2X/\lambda$, where X is the length of the traverse and λ is the acoustic wavelength. Experimental investigations have shown that traverse averaging is as good or better than discrete point averaging, in addition to frequently being a time saving procedure.[2]

The final statistical variable which must be considered in reverberant field power measurements is that due to variations in source position. The acoustic power output of any given source is a function of the acoustic impedance presented to it by the surrounding medium. The modal patterns set up in a reverberation room may increase or decrease this impedance depending upon source location and upon source frequency in relation to room modal frequencies. Lyon (14) determined the theoretical variance in average pure tone sound power with changes in source position

---

[2]This idea is from the paper "Experimental Evaluation of Microphone Traverses in a Reverberant Room" presented to the Acoustical Society of America by C. E. Ebbing and D. J. Ingalls on November 7, 1969.

for a monopole type point source. His procedure and results will be discussed briefly in the next chapter. Computer studies (9, 15) have confirmed Lyon's results and have also shown that the greatest contribution to the variance comes from source positions within one-quarter of a wavelength of the chamber walls, floor, and ceiling.

Ebbing (9) and Tichy[3] have obtained lower variances by installing a rotating diffuser in the reverberation room to continuously shift the modal patterns. By use of a properly designed diffuser, two and even threefold decreases in variance have been obtained.

With the major sources of error in reverberant room power measurements defined, the total variance is simply the sum of all individual variances (2). Thus, to predict the total uncertainty in a given power measurement, the variances due to all significant sources of error must be thoroughly understood. Once understood, of course, this total uncertainty can be decreased to an acceptable level by the choice of sufficient measurement locations.

---

[3] J. Tichy presented the paper "The Effect of Rotating Vanes on the Sound Field in Reverberation Chambers at Single Frequencies" to the Acoustical Society of America on November 3, 1970.

3. POINT SOURCE THEORY

The statistics of power injection associated with a monopole type point source in a diffuse field already exist in the literature. This theory is briefly reviewed in this chapter due to the fact that the finite source development in this study is derived as an extension of point source theory.

From Maling's (15) development of a harmonic point source in a reverberation room, the sound pressure at any point (x,y,z) due to a monopole type source located at point (x_s, y_s, z_s) is given by

$$P(x,y,z,t) = \frac{8i\rho ck(Qoe^{-i\omega t})}{V} \sum_m \frac{\psi_m(x,y,z)\psi_m(x_s,y_s,z_s)}{(k^2-k_m^2) + \frac{2i\beta kS}{V}} \quad , \tag{3.1}$$

where

ψ_m = modal amplitude function for a point source,

$Qoe^{-i\omega t}$ = source volume velocity,

ω = source angular frequency,

t = time,

k, k_m = excitation and modal wave numbers, respectively,

β = damping coefficient,

ρ = density of air,

c = speed of sound in air,

V = volume of room,

S = surface area of room.

Evaluation of equation (3.1) at the surface of the source and division by the source volume velocity yields the input acoustic impedance of the source. This acoustic impedance indicates the reaction of the acoustic medium upon the vibratory motion of the source. The real part of this impedance, the acoustic resistance R, is associated with the dissipation of acoustic energy. Due to the fact that the acoustic power radiated by a source is equal to the rate at which work is done against the acoustic resistance, this resistance governs the sound power output of the source. Therefore, determination of the variance of input acoustic resistance due to changes in source position is analogous to determining the actual variance in source power. The expression for the input acoustic resistance of a harmonic point source is

$$R(x_s,y_s,z_s) = \frac{16\rho c k^2 \beta S}{V^2} \sum_m \frac{\psi_m^2 (x_s,y_s,z_s)}{(k^2-k_m^2)^2 + (\frac{2k\beta S}{V})^2} \quad . \tag{3.2}$$

Using equations adapted from Rice (18), Lyon utilized an expression similar to equation (3.2) to obtain the mean acoustic resistance and the variance of acoustic resistance normalized to the mean for a pure tone point source in a diffuse field. The results are

$$m_R = \frac{k^2 \rho c}{4\pi} \quad , \tag{3.3}$$

$$\frac{\sigma_R^2}{m_R^2} = \sigma_N^2 = \frac{2.7}{16} \frac{1}{M} \quad , \tag{3.4}$$

where

m_R = mean acoustic resistance,

σ_R^2 = variance of acoustic resistance or acoustic power,

σ_N^2 = normalized variance of acoustic resistance or acoustic power,

M = modal overlap of room.

The modal overlap function M is given by

$$M = \frac{\pi k n(k) \eta}{2} \quad , \tag{3.5}$$

where $n(k)$ is the wave number modal density of the room and η is the damping loss factor.

It should be noted that the mean acoustic resistance in equation (3.3) is equal to the acoustic resistance of a point source in a free field. This means that the average acoustic power output of a point source in a diffuse field is equal to its power output in a free field.

The normalized variance in equation (3.4) can be put in a more practical form by expressing the modal overlap in equation (3.5) in terms of measurable acoustic properties. The damping loss factor is assumed to be equal to (23)

$$\eta = \frac{2.2}{fT} \quad , \tag{3.6}$$

where f is the source frequency in Hertz. The modal density of a rectangular room in terms of the wave number is (3)

$$n(k) = \frac{k^2 V}{2\pi^2} \quad . \tag{3.7}$$

Substituting equations (3.6) and (3.7) into equation (3.5) the following expression for M is obtained:

$$M = \frac{4.4\pi^2 f^2 V}{c^3 T} \quad . \tag{3.8}$$

This expression for M is then substituted into equation (3.4) to give an expression for the normalized variance in terms of measurable properties. The result is

$$\sigma_N = \frac{7.39 \times 10^3}{f} \left(\frac{T}{V}\right)^{1/2} \quad . \tag{3.9}$$

In order to get a better grasp of equation (3.9), assume the existence of a reverberation room of scale length L, so that $V \cong L^3$. Then, from equation (2.1)

$$T = 0.0081 \frac{V}{\bar{\alpha}}^{1/3} \quad . \tag{3.10}$$

Substitution of equation (3.10) into equation (3.9) yields

$$\sigma_N = \frac{665}{\bar{\alpha}^{1/2}} \frac{1}{fV^{1/3}} \quad , \tag{3.11}$$

which is graphed in Figure 3.1. This graph clearly shows the effects of absorption coefficient, frequency, and room volume upon the standard deviation of pure tone sound power for two typical values of $\bar{\alpha}$. An increase in either average absorption coefficient, frequency, or room volume decreases the normalized standard deviation of power.

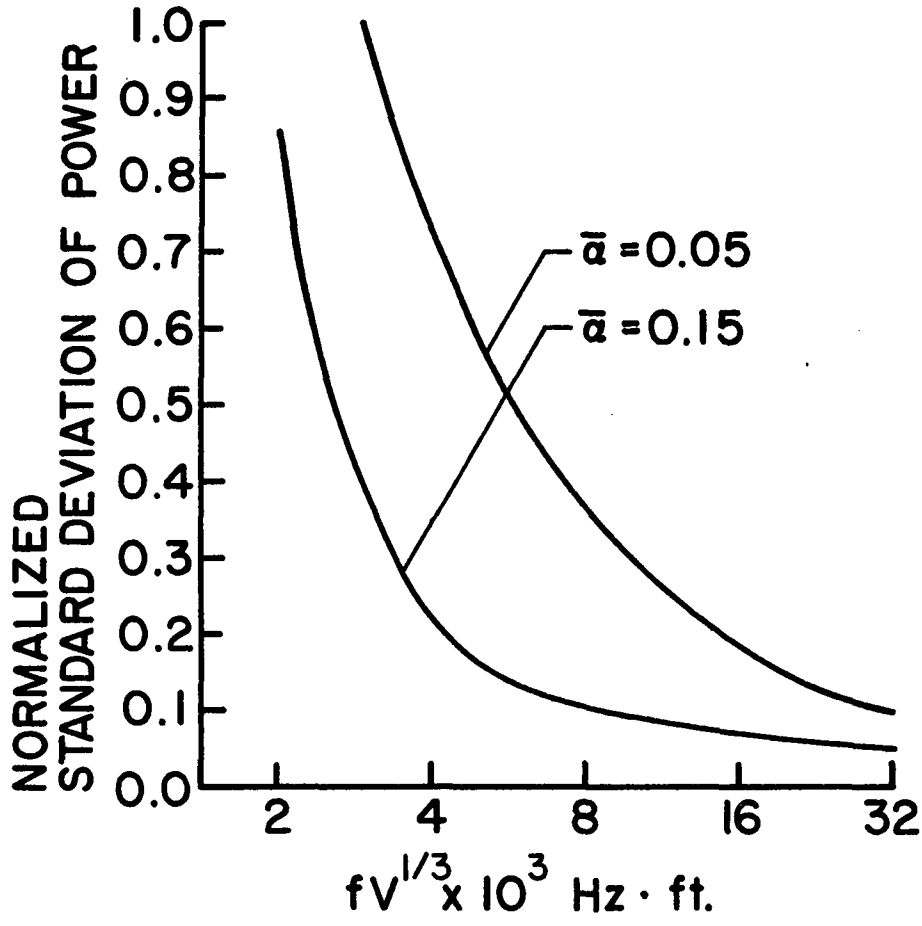

3.1 Uncertainty of sound power output at a single arbitrary source position for a pure tone point source

4. FINITE SOURCE THEORY

4.1 Mean Acoustic Resistance

The previous analysis for a point source can now be used in part to determine the statistics of power injection for a monopole type source of finite size. The finite source is modeled as a baffled square piston of dimension d oriented parallel to the y-z plane as shown in Figure 4.1. The location of this piston in the reverberation room is made with reference to the piston's geometric center which is given the arbitrary designation (x_s, y_s, z_s). Considering this finite source to be composed of a number of point sources in phase, the desired input acoustic resistance for the source model can be obtained by averaging the acoustic resistance of each constituent point source, as given by equation (3.2), over the finite source area. This averaging process is represented by

$$\hat{R}(x_s,y_s,z_s) = \frac{1}{d^2} \int_{A_s} R(x_s,y_s,z_s)\, dA_s \quad , \tag{4.1}$$

where $\hat{R}$ is the average acoustic resistance of the finite source model and A_s is the surface area.

In order to perform the integration indicated in equation (4.1), an expression is needed for the point source modal amplitude function ψ_m in relation to the source location. For a rectangular room, this function is given by (24)

$$\psi_m = \cos k_x x_s \cos k_y y_s \cos k_z z_s \quad , \tag{4.2}$$

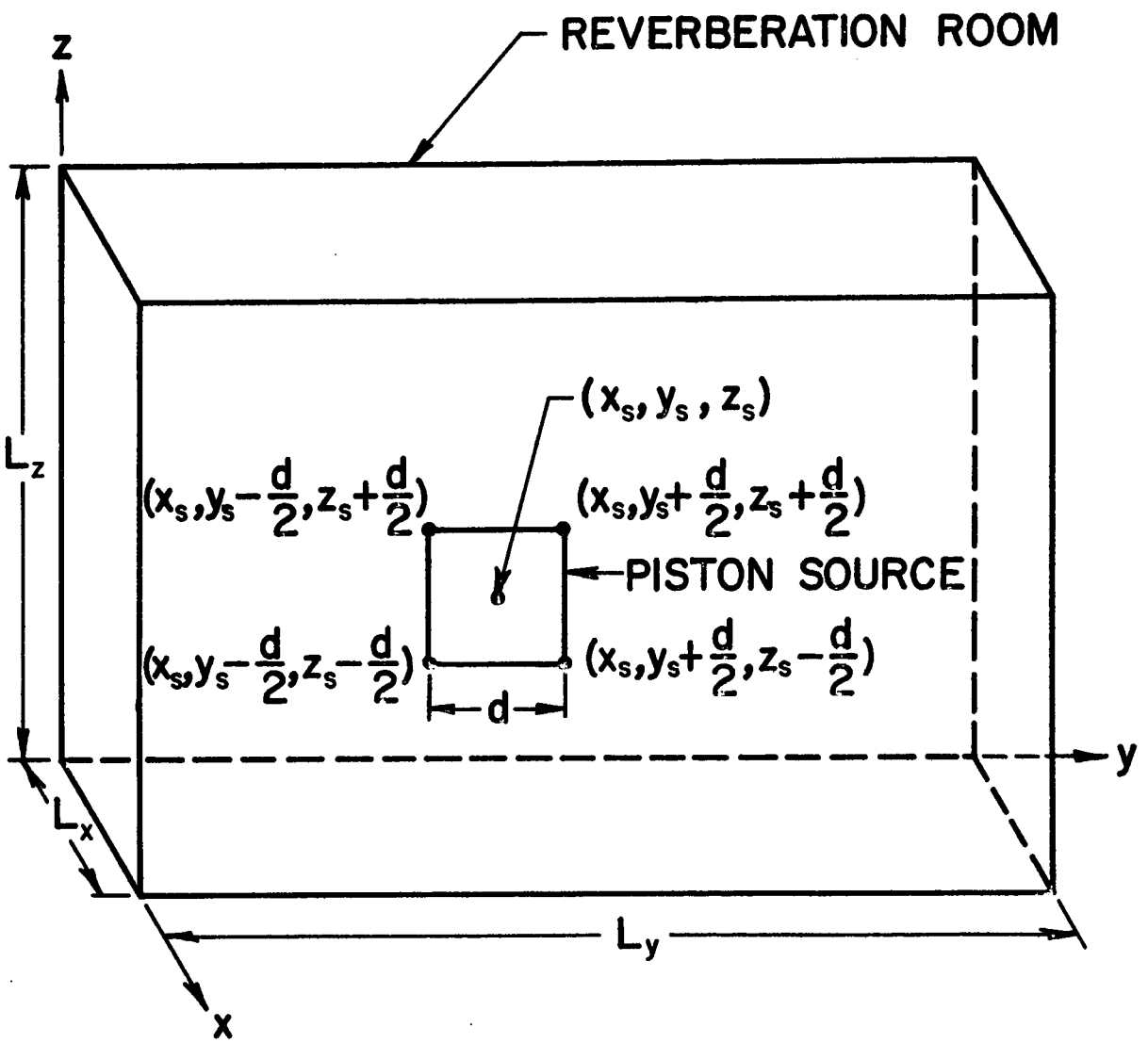

4.1 Finite source model positioned in a reverberation room

where k_x, k_y, and k_z are the components of the modal wave number k_m in the x, y, and z directions, respectively. Substitution of equations (3.2) and (4.2) into equation (4.1), with the establishment of proper limits, yields

$$\hat{R}(x_s,y_s,z_s) = \sum_m \frac{16\rho c k^2 \beta S}{d^2 V^2} \frac{\cos^2 k_x x_s}{(k^2-k_m^2)^2 + (\frac{2k\beta S}{V})^2}$$

$$\int_{y_s-d/2}^{y_s+d/2} \int_{z_s-d/2}^{z_s+d/2} \cos^2 k_y Y' \cos^2 k_z Z' \, dy' dz' \quad , \tag{4.3}$$

where y' and z' are arbitrary variables of integration. The results of the integration are

$$\hat{R}(x_s,y_s,z_s) = \sum_m \frac{16\rho c k^2 \beta S}{d^2 V^2} \frac{\cos^2 k_x x_s}{(k^2-k_m^2)^2 + (\frac{2k\beta S}{V})^2}$$

$$\left\{ \left[\frac{Y'}{2k_y} + \frac{1}{4k_y} \sin 2y' \right]_{k_y(y_s-d/2)}^{k_y(y_s+d/2)} \left[\frac{z'}{2k_z} + \frac{1}{4k_z} \sin 2z' \right]_{k_z(z_s-d/2)}^{k_z(z_s+d/2)} \right\} ,$$

or

$$\hat{R}(x_s,y_s,z_s) = \sum_m \frac{16\rho c k^2 \beta S}{d^2 V^2} \frac{\cos^2 k_x x_s}{(k^2-k_m^2)^2 + (\frac{2k\beta S}{V})^2}$$

$$\left\{ \left[\left(\frac{y_s+d/2}{2} + \frac{\sin 2k_y(y_s+d/2)}{4k_y} \right) - \left(\frac{y_s-d/2}{2} + \frac{\sin 2k_y(y_s-d/2)}{4k_y} \right) \right] \right.$$

$$\left[\left(\frac{z_s+d/2}{2} + \frac{\sin 2k_z(z_s+d/2)}{4k_z} \right) - \left(\frac{z_s-d/2}{2} + \right. \right.$$

$$\left. \left. \frac{\sin 2k_z(z_s-d/2)}{4k_z} \right) \right] \Bigg\} \quad . \tag{4.4}$$

In order to simplify equation (4.4) for easier manipulation, let

$$A = \frac{16\rho c k^2 \beta S}{V^2} \quad , \tag{4.5}$$

$$B = (k^2 - k_m^2)^2 + \left(\frac{2k\beta S}{V}\right)^2 \quad . \tag{4.6}$$

Reduction of equation (4.4) then results in

$$\hat{R}(x_s,y_s,z_s) = \sum_m \frac{A}{d^2 B} \cos^2 k_x x_s$$

$$\left\{ \left[\frac{d}{2} + \frac{\sin 2k_y(y_s+d/2)}{4k_y} - \frac{\sin 2k_y(y_s-d/2)}{4k_y} \right] \right.$$

$$\left. \left[\frac{d}{2} + \frac{\sin 2k_z(z_s+d/2)}{4k_z} - \frac{\sin 2k_z(z_s-d/2)}{4k_z} \right] \right\} . \tag{4.7}$$

From a knowledge of trigonometric relationships,

$$\sin 2(p+q) - \sin 2(p-q) = \sin 2p \cos 2q$$

$$+ \cos 2p \sin 2q - \sin 2p \cos 2q$$

$$+ \cos 2p \sin 2q \quad ,$$

and

$$\cos 2p = 2 \cos^2 p - 1.$$

Thus,

$$\sin 2(p+q) - \sin 2(p-q) = 4 \cos^2 p \sin 2q - 2 \sin 2q \quad . \qquad (4.8)$$

Utilization of the relationship of equation (4.8) in equation (4.7) yields

$$\hat{R}(x_s,y_s,z_s) = \sum_m \frac{A}{d^2 B} \cos^2 k_x x_s$$

$$\left\{ \left[\frac{d}{2} + \left(\frac{2 \cos^2 k_y y_s \sin k_y d - \sin k_y d}{2k_y} \right) \right] \right.$$

$$\left. \left[\frac{d}{2} + \left(\frac{2 \cos^2 k_z z_s \sin k_z d - \sin k_z d}{2k_z} \right) \right] \right\} \quad . \qquad (4.9)$$

The bracketed quantity in equation (4.9) can finally be put into non-dimensionalized form so that the average acoustic resistance of the finite source model can be expressed either in factor form by

$$\hat{R}(x_s,y_s,z_s) = \sum_m \frac{A}{B} \cos^2 k_x x_s$$

$$\left\{ \left[\frac{1}{2} \left(\frac{k_y d - \sin k_y d}{k_y d} \right) + \cos^2 k_y y_s \frac{\sin k_y d}{k_y d} \right] \right.$$

$$\left. \left[\frac{1}{2} \left(\frac{k_z d - \sin k_z d}{k_z d} \right) + \cos^2 k_z z_s \frac{\sin k_z d}{k_z d} \right] \right\} , \qquad (4.10)$$

or in expanded form by

$$\hat{R}(x_s,y_s,z_s) = \sum_m \frac{A}{B} \left\{ \frac{1}{4} \cos^2 k_x x_s \left(\frac{k_y d - \sin k_y d}{k_y d}\right) \right.$$

$$\left(\frac{k_z d - \sin k_z d}{k_z d}\right) + \frac{1}{2} \cos^2 k_x x_s \cos^2 k_z z_s \frac{\sin k_z d}{k_z d}$$

$$\left(\frac{k_y d - \sin k_y d}{k_y d}\right) + \frac{1}{2} \cos^2 k_x x_s \cos^2 k_y y_s \frac{\sin k_y d}{k_y d}$$

$$\left(\frac{k_z d - \sin k_z d}{k_z d}\right) + \cos^2 k_x x_s \cos^2 k_y y_s \cos^2 k_z z_s$$

$$\left. \frac{\sin k_y d}{k_y d} \frac{\sin k_z d}{k_z d} \right\} . \qquad (4.11)$$

If we represent the bracketed quantity in equation (4.11) by the symbol ϕ_m^2 and recall the values of A and B from equations (4.5) and (4.6), the finite source acoustic resistance takes on the form

$$\hat{R}(x_s,y_s,z_s) = \frac{16\rho c k^2 \beta S}{V^2} \sum_m \frac{\phi_m^2}{(k^2-k_m^2)^2 + \left(\frac{2\beta k S}{V}\right)^2} , \qquad (4.12)$$

which is very similar to the acoustic resistance for a point source given by equation (3.2). The only difference is the replacement of ψ_m^2 for a point source by ϕ_m^2 must represent the squared modal amplitude function for the finite source model.

It should be noted that in the limit as the finite source dimension d approaches zero, equation (4.12) reduces to

$$\lim_{d\to 0} \hat{R}(x_s,y_s,z_s) = \frac{16\rho c k^2 \beta S}{V^2} \sum_m \frac{\cos^2 k_x x_s \cos^2 k_y y_s \cos^2 k_z z_s}{(k^2-k_m^2)^2 + (\frac{2\beta k S}{V})^2}$$

$$= \frac{16\rho c k^2 \beta S}{V^2} \sum_m \frac{\psi_m^2}{(k^2-k_m^2)^2 + (\frac{2k\beta S}{V})^2} \quad .$$

Thus, as the size of the finite source becomes very small, the average finite source acoustic resistance reduces to that for a point source.

A graphical sketch of equation (4.12) would exhibit randomly spaced peaks as shown in Figure 4.2, resembling a sequence of pulses from a random signal generator. The peak amplitudes would depend upon the modal amplitude function ϕ_m^2 and upon the source location, which is assumed to be equally probable at all points in the room. Furthermore, it has been assumed that all modes in a given frequency interval have approximately the same damping coefficient β. This is equivalent to saying that all the peaks or pulses in a given interval have nearly the same shape, and β is not modal dependent.

The statistics of pulse sequences with Poisson separations have been studied at length by Rice (18), thereby making expressions for the mean and variance of such sequences readily available. Therefore, for the entirety of this theoretical derivation, the modal peaks will be assumed to exhibit this type of statistical distribution.

Using Rice's formula, as adapted for special use in acoustic environments by Lyon, the mean value of the acoustic resistance in

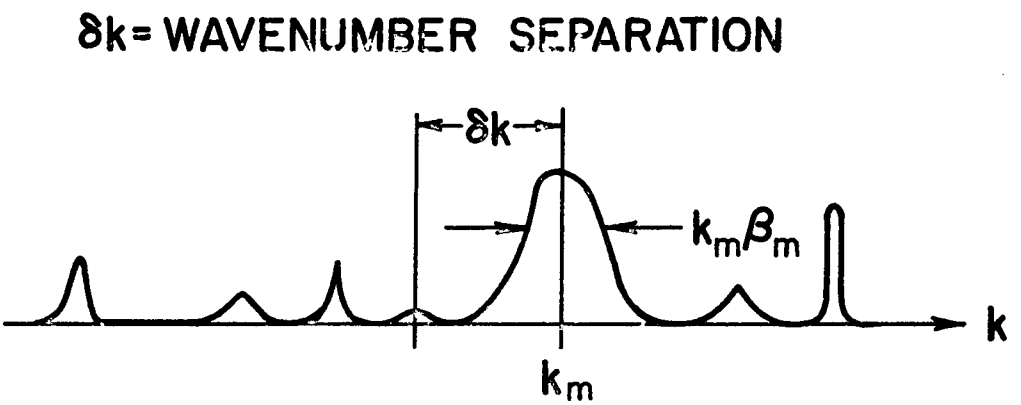

4.2 Graph of acoustic resistance in a room

equation (4.12) is given by

$$M_R = \frac{16\rho c k^2 \beta S}{V^2} \int_0^\infty \frac{\langle \phi_m^2 \rangle \, n(k_m) \, dk_m}{(k^2 - k_m^2)^2 + \left(\frac{2k\beta S}{V}\right)^2} \quad . \tag{4.13}$$

The quantity $\langle \phi_m^2 \rangle$ represents the spatial average of the squared finite source modal amplitude function. This spatial average is performed over all possible source positions in the room volume and can be represented by

$$\langle \phi_m^2 \rangle = \frac{1}{V} \int_0^{L_x} \int_0^{L_y} \int_0^{L_z} \phi_m^2 \, dx_s \, dy_s \, dz_s \quad , \tag{4.14}$$

where L_x, L_y, and L_z are the room dimensions in the three coordinate directions.

Recall from equation (4.11) that

$$\phi_m^2 = \frac{1}{4} \cos^2 k_x x_s \left(\frac{k_y d - \sin k_y d}{k_y d}\right)\left(\frac{k_z d - \sin k_z d}{k_z d}\right)$$

$$+ \frac{1}{2} \cos^2 k_x x_s \cos^2 k_z z_s \frac{\sin k_z d}{k_z d} \left(\frac{k_y d - \sin k_y d}{k_y d}\right)$$

$$+ \frac{1}{2} \cos^2 k_x x_s \cos^2 k_y y_s \frac{\sin k_y d}{k_y d} \left(\frac{k_z d - \sin k_z d}{k_z d}\right)$$

$$+ \cos^2 k_x x_s \cos^2 k_y y_s \cos^2 k_z z_s \frac{\sin k_y d}{k_y d} \frac{\sin k_z d}{k_z d} \quad . \tag{4.15}$$

Again for simplicity in manipulation, make the following substitutions in equation (4.15):

$$D = \frac{k_y d - \sin k_y d}{k_y d} \quad , \tag{4.16a}$$

$$E = \frac{k_z d - \sin k_z d}{k_z d} \quad , \tag{4.16b}$$

$$G = \frac{\sin k_y d}{k_y d} \quad , \tag{4.16c}$$

$$H = \frac{\sin k_z d}{k_z d} \quad . \tag{4.16d}$$

These substitutions then enable one to rewrite equation (4.14) as

$$\langle \phi_m^2 \rangle = \frac{1}{V} \int_0^{L_x} \int_0^{L_y} \int_0^{L_z} \left[\frac{DE}{4} \cos^2 k_x x_s + \frac{DH}{2} \cos^2 k_x x_s \cos^2 k_z z_s + \frac{EG}{2} \cos^2 k_x x_s \cos^2 k_y y_s + GH \cos^2 k_x x_s \cos^2 k_z z_s \right] dx_s \, dy_s \, dz_s \quad .$$

The integration is now carried out to give

$$\langle \phi_m^2 \rangle = \frac{1}{8} [DE + DH + EG + HG] \quad . \tag{4.17}$$

Referring to the expressions for D, E, G, and H from equations (4.16a), (4.16b), (4.16c), and (4.16d), respectively, it can be shown that in the limit as d approaches zero,

$$D \text{ and } E \to 0 \quad , \tag{4.18a}$$

$$G \text{ and } H \to 1 \quad , \tag{4.18b}$$

and therefore,

$$\lim_{d \to 0} \langle \phi_m^2 \rangle = \frac{1}{8} \quad .$$

As might be expected, this limiting value of $\langle \phi_m^2 \rangle$ is equal to the value of $\langle \psi_m^2 \rangle$ obtained by Lyon for a point source. Thus, the spatial average of the squared modal amplitude function for the finite source approaches that for a point source as the finite source dimension becomes very small.

This value of $\langle \phi_m^2 \rangle$, however, instead of being a function of the modal wave number k_m, is a function of the components of the modal wave number in each coordinate direction $[k_x, k_y, k_z]$. Substitution of equation (4.17) into equation (4.13), therefore, does not result in an integrand amenable to direct integration with respect to the variable of integration k_m. A means of transforming equation (4.17) to an expression depending solely upon k_m and not its vector components is definitely needed.

One means of performing this transformation is through the utilization of a wave number lattice diagram. The relationship

$$k_m^2 = k_x^2 + k_y^2 + k_z^2$$

suggests that each modal wave number may be represented as a vector in wave number space (16), having components k_x, k_y, and k_z. Each of these

components can be expressed in terms of the properties of the reverberant enclosure by

$$k_x = \frac{n_x \pi}{L_x} \quad , \tag{4.19a}$$

$$k_y = \frac{n_y \pi}{L_y} \quad , \tag{4.19b}$$

$$k_z = n_z \pi / L_z \quad , \tag{4.19c}$$

where n_x, n_y, and n_z represent the actual mode numbers in the x, y, and z directions, respectively. A normal mode of vibration can, therefore, be represented as a point in wave number space, with the x component of this point being some integral multiple of π/L_x, the y component some multiple of π/L_y, and the z component some multiple of π/L_z. Such a wave number lattice for a rectangular room is shown in Figure 4.3. All normal modes having a characteristic wave number equal to or less than k_m are included in an octant of this space of radius k_m.

This point lattice representation of the normal modes of a room can prove quite useful for making two approximations necessary to this study. First of all, the lattice can be used to obtain an equation approximating the number of modes existent in a particular frequency interval. Each lattice point is assumed to occupy a space of dimensions π/L_x, π/L_y, and π/L_z and of volume π^3/V. The number of modes N below a given wave number k_m can then be determined by dividing the volume of an octant of radius k_m $[\pi k_m^3/6]$ by π^3/V. This yields

$$N = \frac{k_m^3 V}{6\pi^2} \quad . \tag{4.20}$$

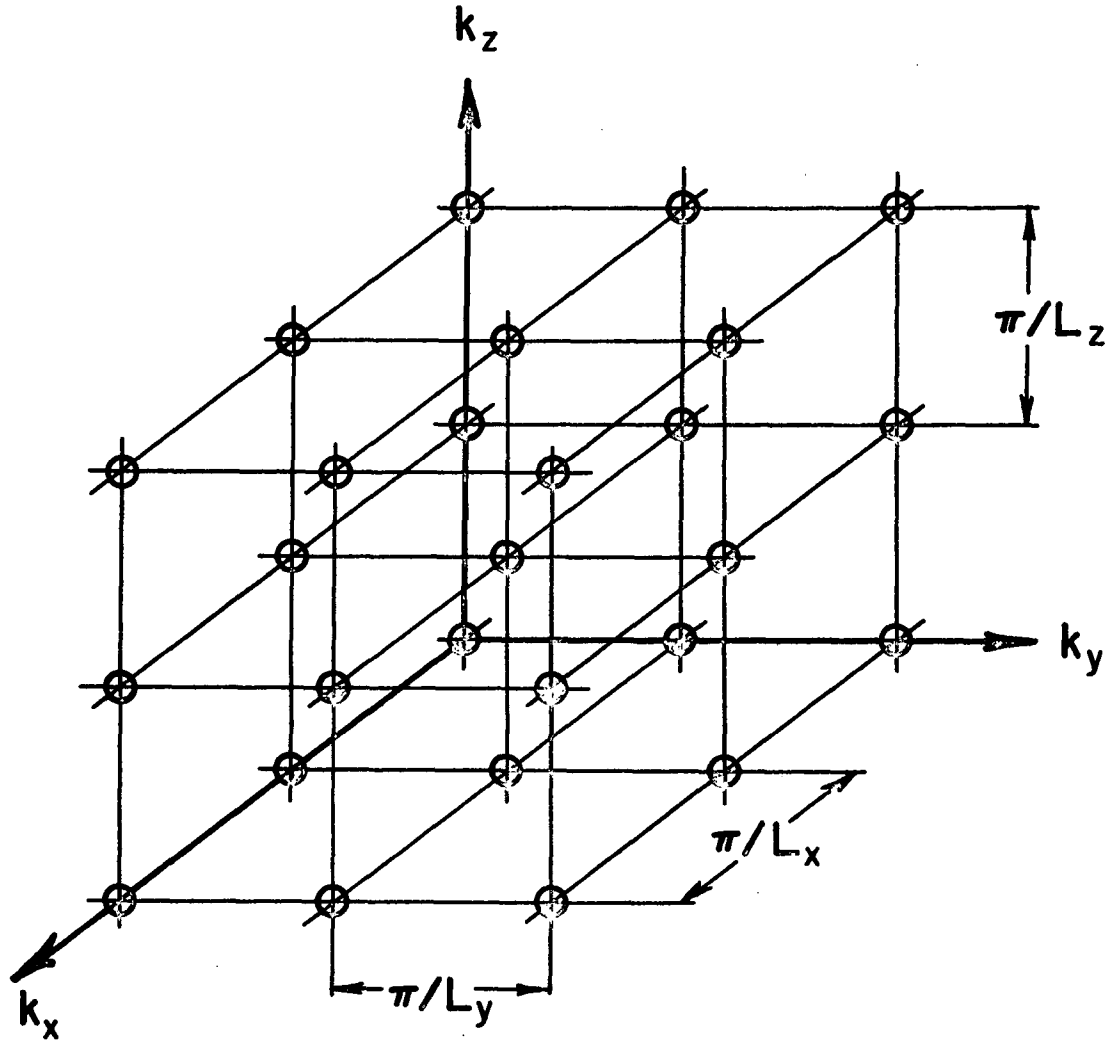

4.3 Normal modes represented as a wave number lattice

A still more useful quantity can be obtained by differentiating equation (4.20) with respect to k_m. This yields the number of normal modes contained in the wave number interval dk_m, centered at k_m. The result is

$$\frac{dN}{dk_m} = \frac{k_m^2 V}{2\pi^2} \quad , \tag{4.21}$$

which should be recognized as the approximate modal density $n(k_m)$ of a rectangular reverberation room [equation (3.7)]. An increase in this modal density, either by an increase in wave number [higher frequency] or by an increase in room volume, results in a higher degree of random distribution of sound energy. As discussed in Chapter 2, any elevation in the degree of random distribution serves to improve the diffuse approximation for the reverberant field.

The second important use of the wave number lattice is as a means of expressing equation (4.17) as a function of k_m. This is accomplished through recognition of the fact that the components of any point in the wave number lattice can be expressed in terms of k_m by use of spherical coordinates. The representation of a typical point is shown in Figure 4.4. The results as obtained from the figure are

$$k_x = k_m \sin\theta \cos\gamma \quad , \tag{4.22a}$$

$$k_y = k_m \sin\theta \sin\gamma \quad , \tag{4.22b}$$

$$k_z = k_m \cos\theta \quad . \tag{4.22c}$$

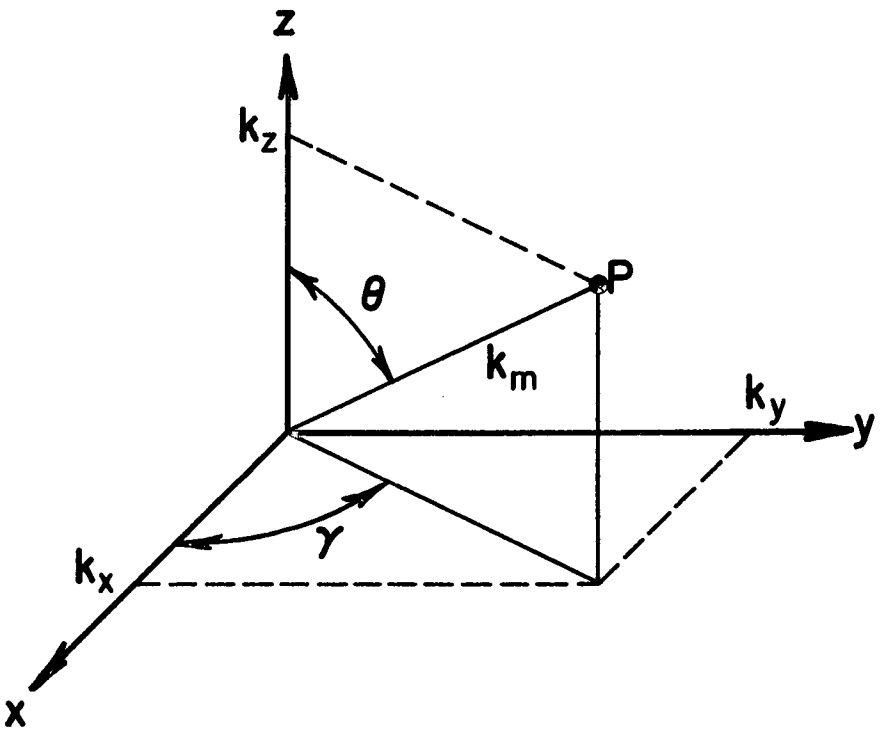

4.4 Representation of the vector k_m in spherical coordinates

Substitution of these coordinate relationships into equations (4.16a), (4.16b), and (4.16c) then results in

$$D = \frac{k_m d \sin\theta \sin\gamma - \sin(k_m d \sin\theta \sin\gamma)}{k_m d \sin\theta \sin\gamma} \quad , \tag{4.23a}$$

$$E = \frac{k_m d \cos\theta - \sin(k_m d \cos\theta)}{k_m d \cos\theta} \quad , \tag{4.23b}$$

$$G = \frac{\sin(k_m d \sin\theta \sin\gamma)}{k_m d \sin\theta \sin\gamma} \quad , \tag{4.23c}$$

$$H = \frac{\sin(k_m d \cos\theta)}{k_m d \cos\theta} \quad . \tag{4.23d}$$

After the insertion of equations (4.23a), (4.23b), (4.23c), and (4.23d) into equation (4.17), the dependence of $\langle\phi_m^2\rangle$ upon k_x, k_y, and k_z is eliminated, but the dependence upon the angular position of k_m in the wave number lattice has been introduced. This new dependence problem, however, can be solved by averaging $\langle\phi_m^2\rangle$ over all possible angular locations of k_m in the lattice.[4] This is equivalent to stating that $\langle\phi_m^2\rangle$ is averaged over the surface of an octant of radius k_m in the wave number

$$\langle\phi_m^2\rangle = \frac{1}{k_m^2 \pi/2} \int_0^{\pi/2} \int_0^{\pi/2} \langle\phi_m^2\rangle k_m^2 \sin\theta \, d\theta \, d\gamma \quad , \tag{4.24}$$

---

[4] This averaging process was suggested by S. N. Yousri and F. J. Fahy, University of Southampton, England.

where $k_m^2\pi/2$ is the surface area of the octant and $k_m^2 \sin\theta\, d\theta\, d\gamma$ is the area of a typical differential element.

Because of the extremely complicated nature of $\langle\phi_m^2\rangle$, equation (4.24) does not lend itself to solution by direct integration methods. However, an approximate integration can easily be performed by treating the integral as a finite double sum and by using numerical solution techniques. A description of the digital computer numerical integration procedure which was devised and utilized is given in Appendix 9.1.

The value of equation (4.24) is obtained as a function if $k_m d$ for values of $k_m d$ from 0.25 to 25.00 at intervals of 0.25. The computer results show $\langle\phi_m^2\rangle$ to be a constant equal to 1/8 for all values of $k_m d$. It should be noted that this computer value of $\langle\phi_m^2\rangle$ is equal to the value of $\langle\psi_m^2\rangle$ for a point source.

Utilizing the result

$$\langle\phi_m^2\rangle = 1/8$$

in equation (4.13), the following integral for the mean value of acoustic resistance is obtained:

$$m_R = \frac{2\rho c k^2 \beta S}{V^2} \int_0^\infty \frac{n(k_m)\, dk_m}{(k^2-k_m^2)^2 + \left(\frac{2k\beta S}{V}\right)^2} \quad . \tag{4.25}$$

The damping coefficient β in equation (4.25) is related to the wall damping loss factor η by

$$\beta = \frac{k\eta V}{2S} \quad . \tag{4.26}$$

If η is small [<0.1], which it must be for diffuse conditions to be approximated, then the integral in equation (4.25) peaks sharply about $k_m \cong k$, and the following reduction can be made:

$$m_R = \frac{2\rho c \beta S}{V^2} \int_0^\infty \frac{n(k)\, dk_m}{\frac{(k^2 - k_m^2)^2}{k} + \left(\frac{2\beta S}{V}\right)^2} \quad . \tag{4.27}$$

Letting

$$R = \frac{k^2 - k_m^2}{k} \quad ,$$

and

$$dR = \frac{k_m^2 + k^2}{k^2}\, dk_m$$

$$\cong 2\, dk_m \quad ,$$

then equation (4.27) transforms to

$$m_R = \frac{\rho c}{2V}\, n(k) \int_{-\infty}^{\infty} \frac{(2\beta S/V)}{R^2 + \left(\frac{2\beta S}{V}\right)^2}\, dR \tag{4.28}$$

for small damping. Integration of equation (4.28) yields

$$m_R = \frac{\rho c n(k) \pi}{2V} \quad . \tag{4.29}$$

Recalling the approximate value of the modal density of the room n(k) from equation (4.20), the final result for the mean acoustic resistance of the finite source model is

$$m_R = \frac{\rho c k^2}{4\pi} \quad . \tag{4.30}$$

This is exactly the same result as was obtained by Lyon for a point source [equation (3.3)]. Thus, the mean acoustic resistance of the finite source model in a reverberant room is equal to that for a point source in a reverberant room and also equal to that for a point source in the free field.[5]

This result takes on a greater significance if recognition is made of the relationship between average acoustic power and mean acoustic resistance. This relationship is given by

$$W = S^2 \bar{V}^2 m_R ,$$

where

W = average acoustic power,

S = source radiating area,

$\bar{V}^2$ = mean square source velocity.

For monopole type radiation, $S^2 \bar{V}^2$ is equivalent to the source volume velocity squared. Thus, for the case of equal volume velocities, a point source and the finite source model exhibit the same average power output in a diffuse field. Furthermore, this average power is equal to the power output of a point source or the finite source model in a free field. This is to be expected if the reverberant room technique is to be used for measurement of the classic free field acoustic power.

---

[5]The dependence of the mean acoustic resistance upon k^2 [equation (4.20)] for values of ka >> 1 has been questioned by P. K. Baade. However, this result has no influence upon the other significant conclusions in this work.

4.2 Standard Deviation of Acoustic Resistance

As mentioned in Section 4.1, the variance or standard deviation of pulse sequences with Poisson separations has been studied in detail by Rice. Thus, using an equation developed by Rice and adapted for acoustical use by Lyon, the variance of the average acoustic resistance for a finite source [equation (4.12)] is given by

$$\sigma_R^2 = \left(\frac{16\rho c k^2 \beta S}{V^2}\right)^2 \int_0^\infty \frac{\langle \phi_m^4 \rangle \, n(k_m) \, dk_m}{\left[(k^2 - k_m^2)^2 + \left(\frac{2k\beta S}{V}\right)^2\right]^2} \quad . \tag{4.31}$$

The quantity $\langle \phi_m^4 \rangle$ represents the spatial average of the finite source modal amplitude function raised to the fourth power. Referring to equations (4.15), (4.16a), (4.16b), (4.16c), and (4.16d), the value of ϕ_m^2 can be squared and simplified to yield the following result for ϕ^4:

$$\begin{aligned}
\phi_m^4 = {} & \frac{D^2E^2}{16} \cos^4 k_x x_s + \frac{D^2H^2}{4} \cos^4 k_x x_s \cos^4 k_z z_s \\
& + \frac{E^2G^2}{4} \cos^4 k_x x_s \cos^4 k_y y_s + G^2H^2 \cos^4 k_x x_s \cos^4 k_y y_s \cos^4 k_z z_s \\
& + \frac{D^2EH}{4} \cos^4 k_x x_s \cos^2 k_z z_s + \frac{DE^2G}{4} \cos^4 k_x x_s \cos^2 k_x y_s \\
& + DEGH \cos^4 k_x x_s \cos^2 k_y y_s \cos^2 k_z z_s \\
& + DH^2G \cos^4 k_x x_s \cos^4 k_z z_s \cos^2 k_y y_s \\
& + EG^2H \cos^4 k_x x_s \cos^4 k_y y_s \cos^2 k_z z_s \quad .
\end{aligned} \tag{4.32}$$

The spatial average of equation (4.32) over the entire room volume is represented by an expression very similar to equation (4.14). That is,

$$\langle \phi_m^4 \rangle = \frac{1}{V} \int_0^{L_x} \int_0^{L_y} \int_0^{L_z} \phi_m^4 \, dx_s \, dy_s \, dz_s \quad . \tag{4.33}$$

Evaluation of this integral at the limits shown yields

$$\langle \phi_m^4 \rangle = \frac{3}{128} D^2E^2 + \frac{9}{256} D^2H^2 + \frac{9}{256} E^2G^2$$

$$+ \frac{27}{512} G^2H^2 + \frac{3}{16} D^2EH + \frac{3}{16} DE^2G$$

$$+ \frac{3}{32} DEGH + \frac{9}{128} DH^2G + \frac{9}{128} EG^2H \quad . \tag{4.34}$$

From Lyon's point source analysis,

$$\langle \psi_m^4 \rangle = (3/8)^3 \quad . \tag{4.35}$$

Therefore, in anticipation of comparing equation (4.34) to equation (4.35), the quantity $(3/8)^3$ is factored out of equation (4.34) to give

$$\langle \phi_m^4 \rangle = \left(\frac{3}{8}\right)^3 \quad \frac{4}{9} D^2E^2 + \frac{2}{3} D^2H^2 + \frac{2}{3} E^2G^2$$

$$+ G^2H^2 + \frac{8}{9} D^2EH + \frac{8}{9} DE^2G$$

$$+ \frac{16}{9} DEGH + \frac{4}{3} DH^2G + \frac{4}{3} EG^2H \quad . \tag{4.36}$$

Recalling once again the results of equations (4.18a) and (4.18b), it can be shown that

$$\lim_{d \to o} \langle \phi_m^4 \rangle = \left(\frac{3}{8}\right)^3 ,$$

which equals the result shown in equation (4.35). Thus, as should now be expected, the quantity $\langle \phi_m^4 \rangle$ for the finite size model approaches $\langle \psi_m^4 \rangle$ for a point source as the finite source dimension becomes very small.

Just as in the previous analysis of the mean, $\langle \phi_m^4 \rangle$ is a function of k_x, k_y, and k_z rather than the desired k_m. The substitution of equation (4.34) into equation (4.31), therefore, leads to an integral which is difficult to evaluate by direct means. Thus, the wave number lattice is once again utilized to express $\langle \phi_m^4 \rangle$ as a function of k_m. This lattice average is given by

$$\langle \phi_m^4 \rangle = \frac{2}{\pi k_m^2} \int_o^{\pi/2} \int_o^{\pi/2} \langle \phi_m^4 \rangle \, k_m^2 \sin\theta \, d\theta \, d\gamma , \tag{4.38}$$

where the expressions developed in equations (4.22a), (4.22b), and (4.22c) have been substituted for k_x, k_y, and k_z.

The integration of this equation, which was once again attacked numerically using a digital computer, resulted in

$$\langle \phi_m^4 \rangle = \frac{27}{256\pi} \xi(k_m d) , \tag{4.39}$$

where ξ is understood to be a numerical value depending upon the magnitude of $k_m d$. A brief description of the computer problem is given in Appendix 9.1.

Substitution of equation (4.39) into equation (4.31) yields the following expression for the variance of acoustic resistance for the finite source model:

$$\sigma_R^2 = \frac{27}{256\pi} \left(\frac{16\rho c\beta S^2}{V^2}\right) \int_0^\infty \frac{k^4 n(k_m)\xi(k_m d)dk_m}{\left[(k^2-k_m^2)^2 + \left(\frac{2k\beta S}{V}\right)^2\right]^2} \quad . \tag{4.40}$$

Upon making the same assumption as in the previous analysis, i.e. the damping is small such that equation (4.40) peaks sharply about $k_m \cong k$, and upon substituting

$$R = \frac{k^2 - k_m^2}{k} \quad ,$$

and

$$dR \cong 2dk_m \quad ,$$

equation (4.40) transforms to

$$\sigma_R^2 = \frac{27}{8\pi} \frac{\rho^2 c^2}{V^2} n(k)\xi(kd) \int_{-\infty}^{\infty} \frac{(2\beta S/V)^2 dR}{\left[R^2 + \left(\frac{2\beta S}{V}\right)^2\right]^2} \quad . \tag{4.41}$$

Integration of equation (4.41), along with the utilization of equation (4.26) yields

$$\sigma_R^2 = \frac{27}{16} \frac{\rho^2 c^2}{kV^2\eta} \; n(k) \; \xi(kd) \quad . \tag{4.42}$$

Finally, normalization of equation (4.42) to the square of the mean, for a point source given by equation (3.30), leads to the expression for the normalized variance of power for the finite source model. The result is

$$\frac{\sigma_R^2}{m_R^2} = \sigma_N^2 = \left(\frac{27}{16}\ \frac{1}{M}\right) \frac{2\xi(kd)}{\pi} \quad , \tag{4.43}$$

where M is the same modal overlap function as was defined in Chapter 3.

It should be immediately evident that the quantity in parentheses in equation (4.43) is exactly the variance of power given in equation (3.4) for a point source. Thus, the variance of power for the finite size source can be put in the more illustrative form,

$$\sigma_{N\ (F.S.)}^2 = \sigma_{N\ (P.S.)}^2 \left[\frac{2\xi(kd)}{\pi} \right] \quad , \tag{4.44}$$

where $\sigma_{N\ (F.S.)}^2$ = variance of power for the finite source model,

$\sigma_{N\ (P.S.)}^2$ = variance of power for a point source.

If equation (4.44) is normalized with respect to $\sigma_{N\ (P.S.)}^2$ and the square root is taken, the resulting equation expresses the ratio of the standard deviation of the finite source model to that of a point source. The result is

$$\frac{\sigma_{N(F.S.)}}{\sigma_{N(P.S.)}} = \left(\frac{2\xi(kd)}{\pi}\right)^{1/2} \quad , \tag{4.45}$$

which is plotted in Figure 4.5 using the values of ξ determined from the computer data. The standard deviation ratio is always less than one and substantially less whenever kd is greater than or equal to three. In terms of acoustic wavelength, this value of kd corresponds to a finite source dimension greater than or equal to one-half an acoustic wavelength. Thus, the most significant result from Figure 4.5 is that the standard deviation for the finite source model is always less than the corresponding value for a point source and substantially less whenever the ratio d/λ is one-half or greater.

In Figure 4.6, the theoretical standard deviation of power for several typical finite size sources is shown plotted against point source theory [equation (3.8)]. For simplicity in representation, the reverberation room is assumed to have a reverberation time of two seconds and a volume of 10,000 cubic feet. It can be seen that as the frequency or the source size increases, the normalized standard deviation of power decreases.

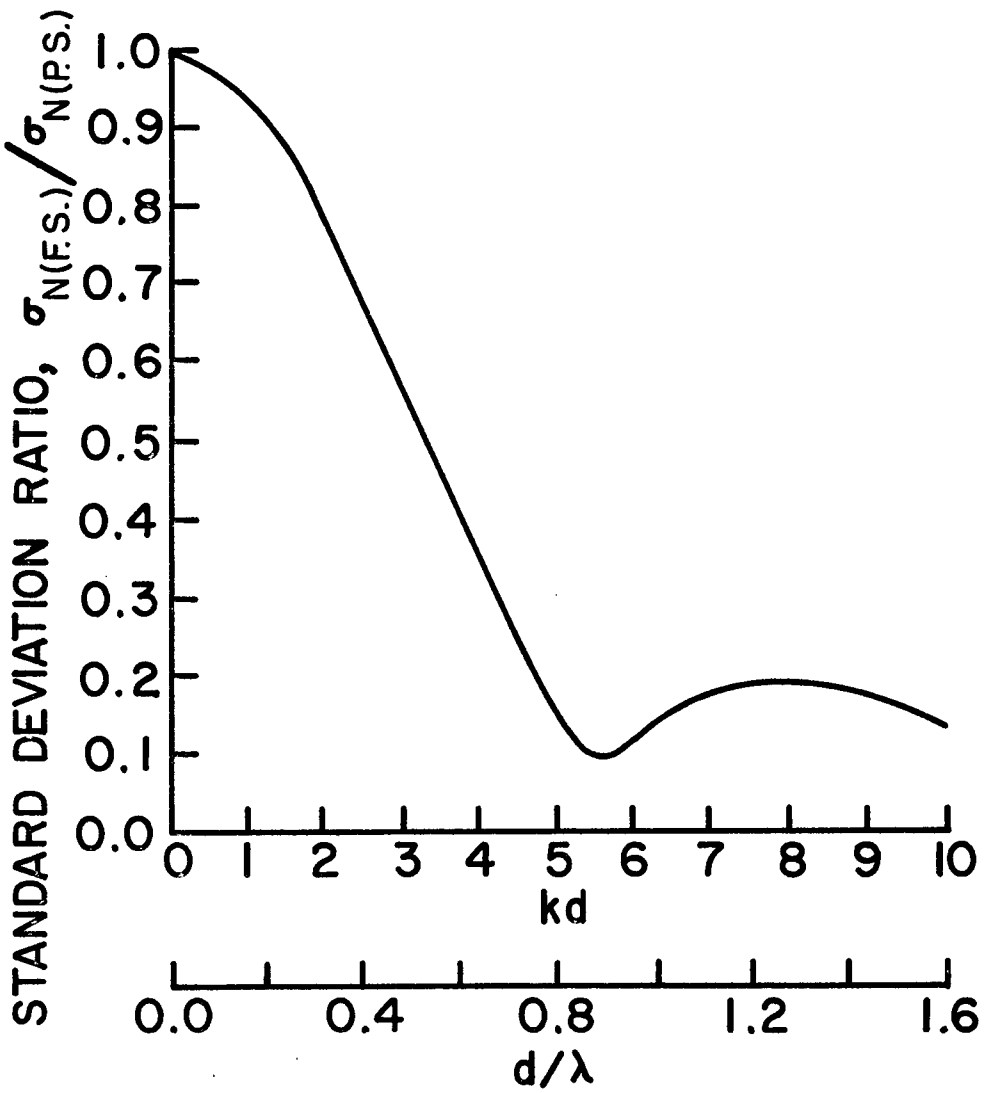

4.5 Dependence of acoustic frequency or wavelength and source dimension on the ratio of the normalized standard deviation of power for a finite source to that for a point source

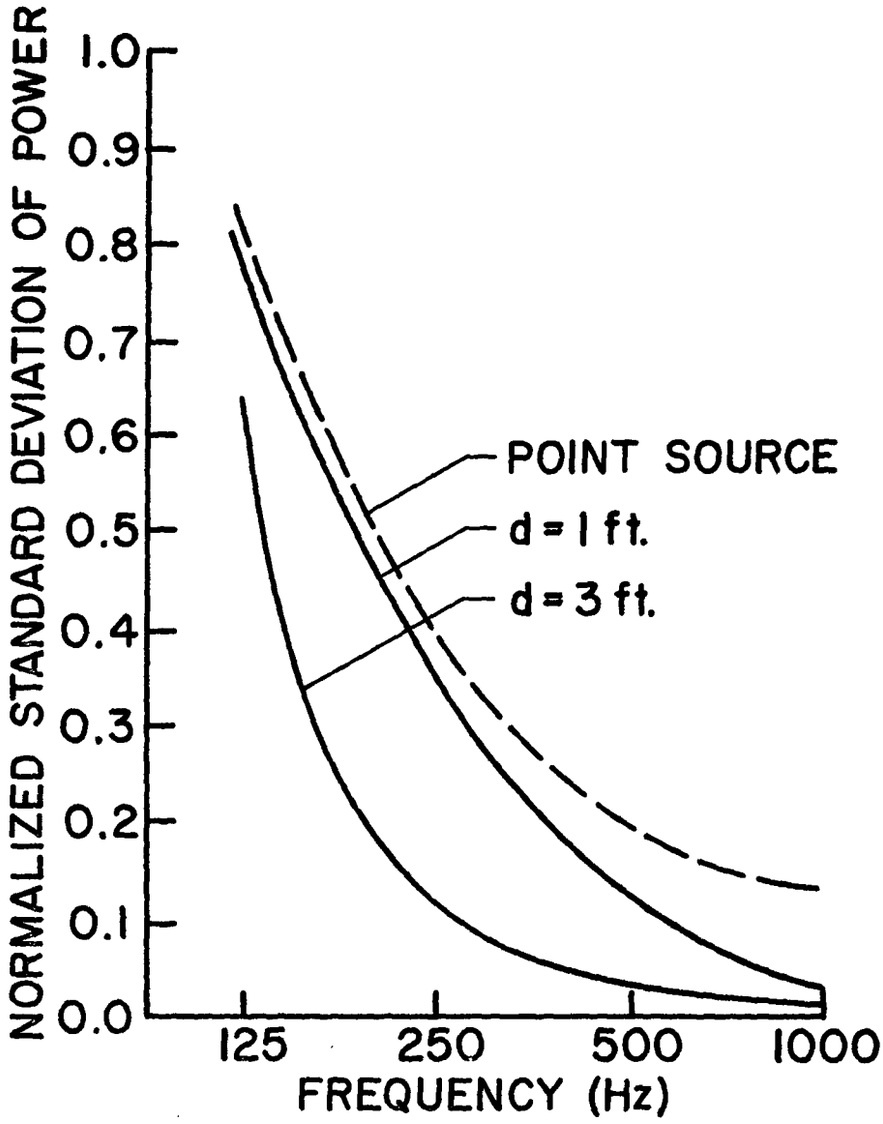

4.6 Graph of the effect of source size on the uncertainty of pure tone sound power using a single source position

5. EXPERIMENTAL INVESTIGATION

5.1 Facilities and Test Setup

The purpose of the experimental portion of this study was to gather data in support of the previous theoretical development for the finite size source model. Since a special reverberation facility was not available for use at the time of this study, the best hard room which could be found among the facilities of the Center for Acoustical Studies was selected for use. The dimensions of this room were 32.0 feet long by 26.3 feet wide by 9.6 feet high representing an internal volume of about 8,000 cubic feet. (Two column protrusions, representing a volume of 60 cubic feet, have been subtracted from the total volume.) These dimensions also correspond to a total room surface area for sound absorption of about 2,900 square feet. Three of the room walls were painted cinder block, one wall was cinder block and glass, the floor was linoleum laid on concrete, and the ceiling was suspended acoustic tile with twelve large fluorescent light fixtures. A schematic diagram of this room is shown in Figure 5.1.

One measure of the acoustical condition of the room is the average absorption coefficient of its walls. This parameter can be determined both theoretically using published absorption data and experimentally using Sabine's diffuse room equation. Moreover, a good agreement between these two methods would be at least an indication of diffuse sound conditions.

The theoretical determination of the average absorption coefficient is accomplished using the following well known equation (5.1):

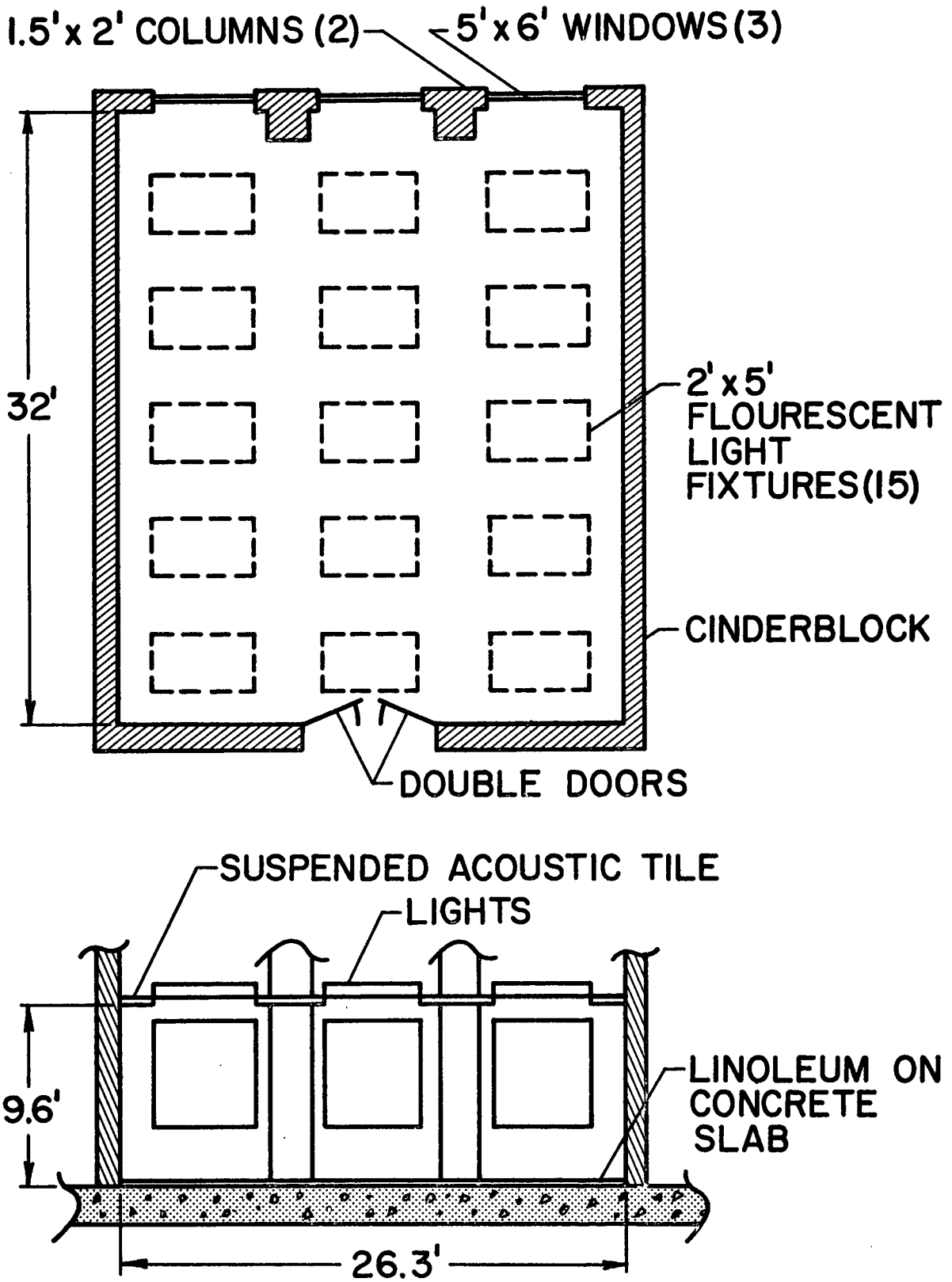

5.1 Plan and elevation cutaway views of the reverberation facility

$$\bar{\alpha} = \frac{\sum_i \alpha_i S_i}{\sum_i S_i} , \qquad (5.1)$$

where $\bar{\alpha}$ = the average absorption coefficient,

α_i = the absorption coefficient of the ith absorbing surface,

S_i = the surface area of the ith absorbing surface.

The α_i's for use in equation (5.1) can be obtained from readily available published data on the absorption coefficients of typical building materials. Table 5.1 shows the absorption coefficient and the associated area of each absorbing surface of the room as a function of the frequencies of interest in this study. The use of the data in this table along with equation (5.1) yields the following theoretical results:

$$\bar{\alpha}_{125} = 0.16,$$

$$\bar{\alpha}_{250} = 0.14,$$

$$\bar{\alpha}_{500} = 0.18,$$

$$\bar{\alpha}_{1000} = 0.22,$$

where the subscripts indicate the calculation frequency. These values indicate that this room would probably be classified as medium hard.

The experimental average absorption coefficients can be calculated using the measured reverberation times of the room. Figure 5.2 shows the experimental setup which was used to make these reverberation measurements for one-third octave bands of random noise. The measured

Table 5.1 Absorption coefficients and surface area of reverberation room materials

Material	Absorption Coefficients				Area (ft^2)
	125	250	500	1000	
Acoustical tile	0.44	0.44	0.61	0.84	660
Cinder block	0.10	0.05	0.06	0.07	1130
Linoleum tile	0.02	0.03	0.03	0.03	840
Window glass	0.09	0.06	0.04	0.03	90
Light fixtures	0.28	0.22	0.17	0.09	180
			Total surface area		2900

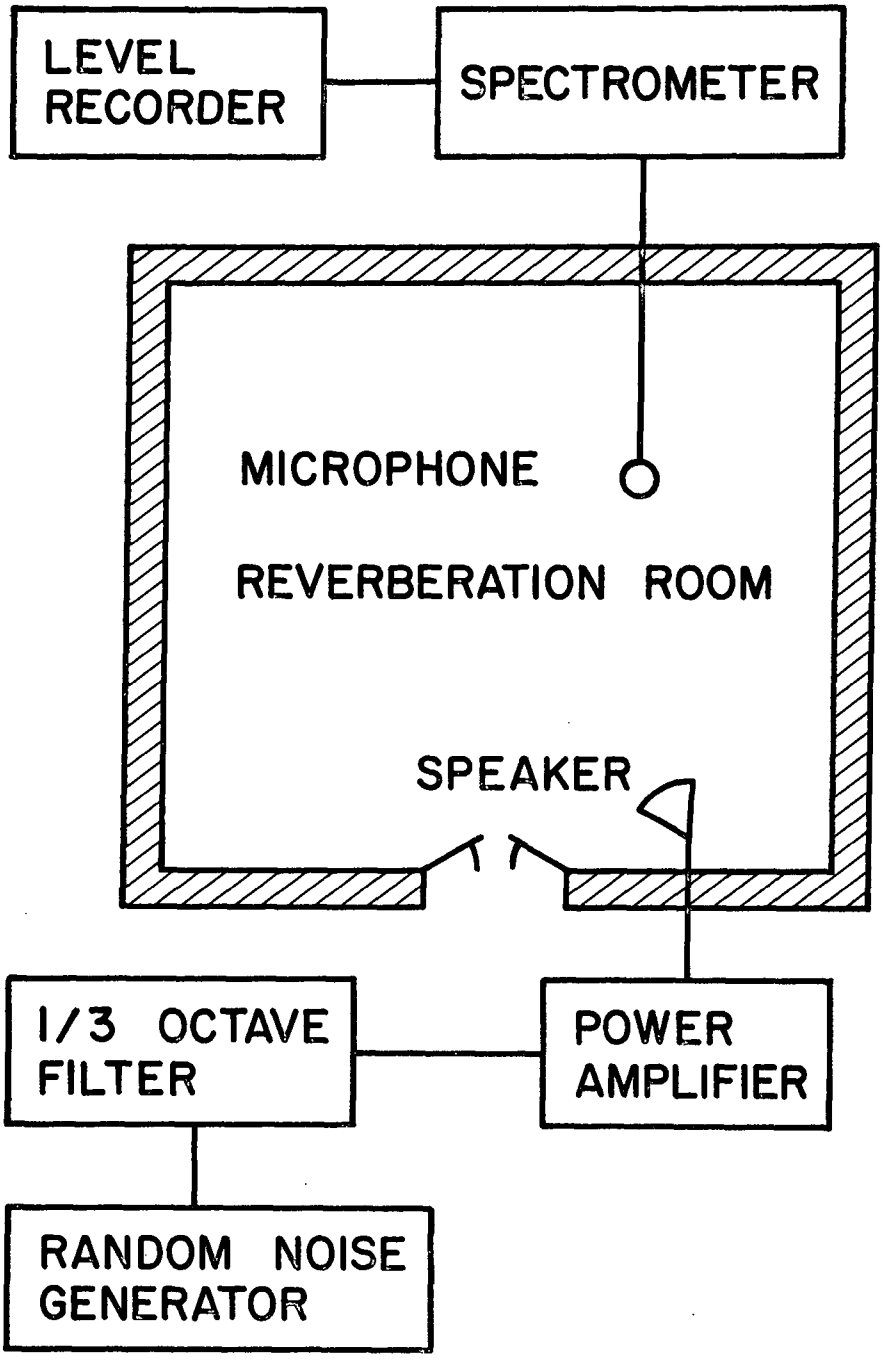

5.2 Test setup for reverberation time measurements

decay times can now be used in conjunction with Sabine's diffuse field relationship [equation (2.1)] to find the desired absorption values. Table 5.2 gives the results of the experimental study, again as a function of the frequencies of interest. The theoretical and experimental values agree fairly well; suggesting the presence of a satisfactory diffuse field.

As stated in Chapter 3, another measure of the room's applicability as a diffuse field is the Schroeder's large room frequency. Having determined the average reverberation time of the room as 1.0 seconds, equation (2.2) yields

$$f_c = 132 \text{ Hz} \quad . \tag{5.2}$$

By Schroeder's theory, a diffuse field exists above this frequency.

The diffusivity of the room was checked in still another way using an eight inch speaker excited by random noise and placed in a corner of the room. Continuous sound level (A) data was taken of this random noise on two seven foot circular arcs at radial distances of ten and twenty feet from the source. The resulting graphs of sound levels, as shown in Figure 5.3, yield a difference in spatial average sound pressure of less than one decibel. This again indicates satisfactory diffuse sound conditions.

The final room evaluation which needed to be made was a measurement of the ambient noise level. Figure 5.4 shows the one-third octave band frequency spectrum which was obtained. All band levels are relatively low except those in the range of 200 Hz and below. More will be said in a later paragraph concerning the precautions which were taken with respect to these relatively high levels in the lower frequency bands.

Table 5.2 Absorption coefficient values calculated using measured reverberation times and Sabine's diffuse field equation

Frequency (Hz)	1/3 Octave Reverberation Time (sec)	Absorption Coefficient
125	1.0	0.13
250	1.0	0.13
500	0.9	0.15
1000	0.8	0.17
Average	1.0	0.14

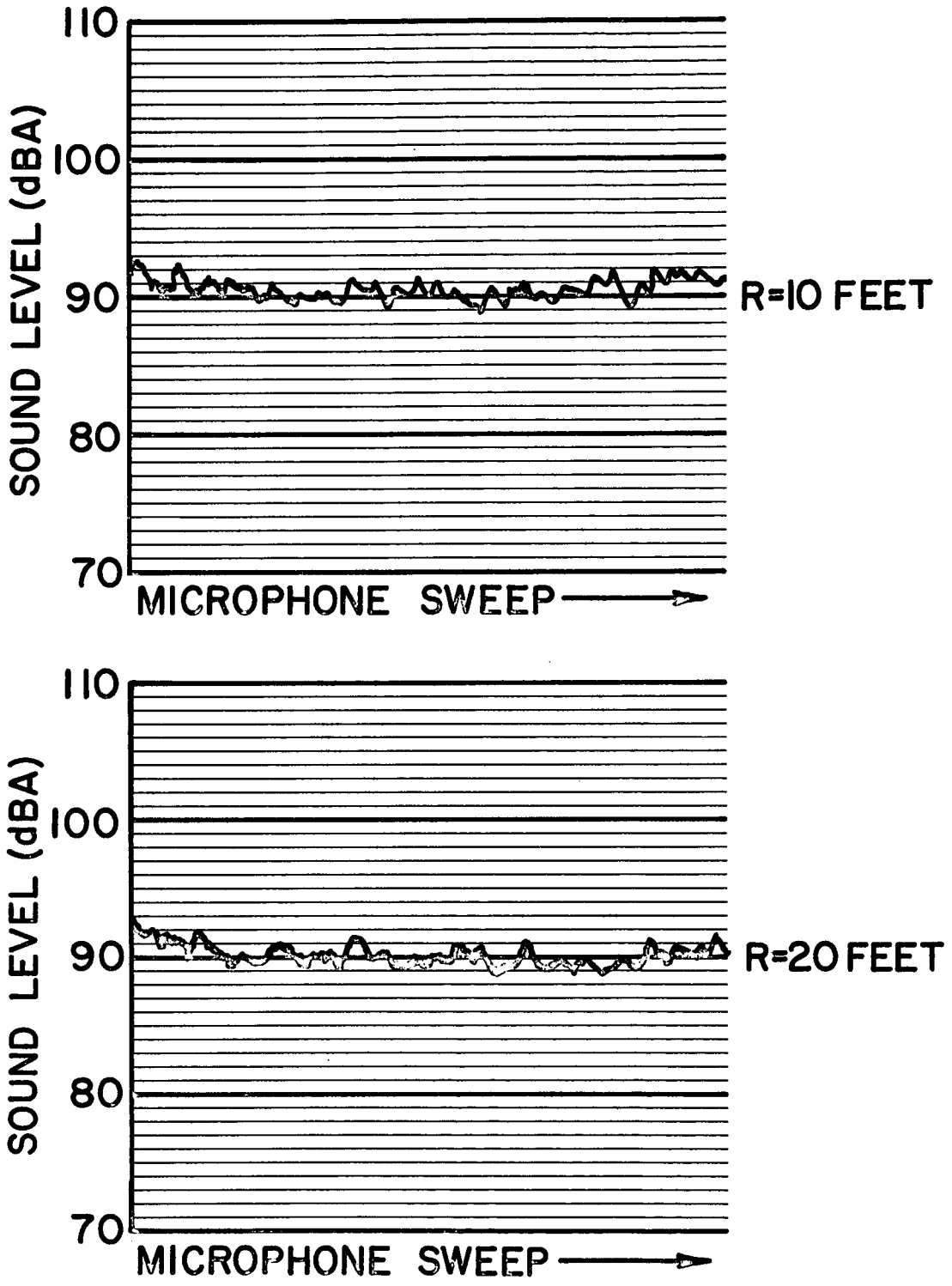

5.3 Continuous sound level (A) graphs at radial distances of 10 and 20 ft from a random noise source in the reverberation room

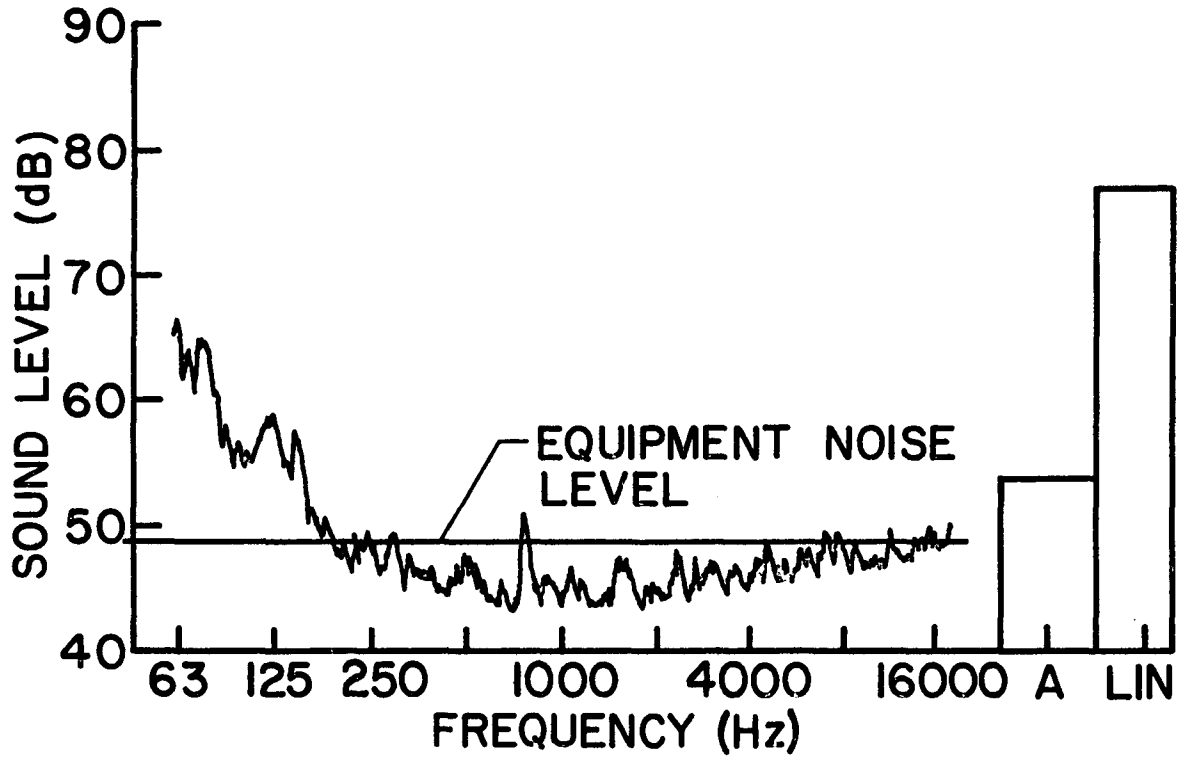

5.4 Ambient noise spectrum in the reverberation room

The basic requirements for the experimental portion of this study included a system to generate the desired pure tones, a system to receive and analyze the resulting room pressure, and a device for recording the resulting data. Figure 5.5 is a schematic diagram of the complete equipment setup used to obtain the necessary data. The noise generation system consisted of a beat frequency or pure tone generator, a power amplifier, an ammeter, a frequency counter, and a sound source. The ammeter was used to keep the current output from the power amplifier constant for each test condition and, thus, regulate the source input power.

The receiving and recording systems consisted of a microphone traversing apparatus, a spectrometer, and a graphic recorder. The traversing device, which was specially designed and constructed for use in this study, was used to facilitate the measurement of the spatial average sound pressure in the room. A complete description of this traverse is presented in Appendix 9.2. The second piece of equipment in this system, the spectrometer, served two purposes. First of all, it provided a means of measuring the actual sound pressure level detected by the microphone, and then it attenuated this microphone signal to a level acceptable for recording purposes. Secondly, through the use of its filtering system, the spectrometer eliminated the rather high components of low frequency ambient noise mentioned previously. The final instrument in the experimental setup was the graphic data recorder. This instrument provided a permanent record of the sound pressure fluctuations as detected by the traversing microphone. Thus, the data could be recorded and then analyzed at a later date. A photograph of the actual equipment setup is shown in Figure 5.6.

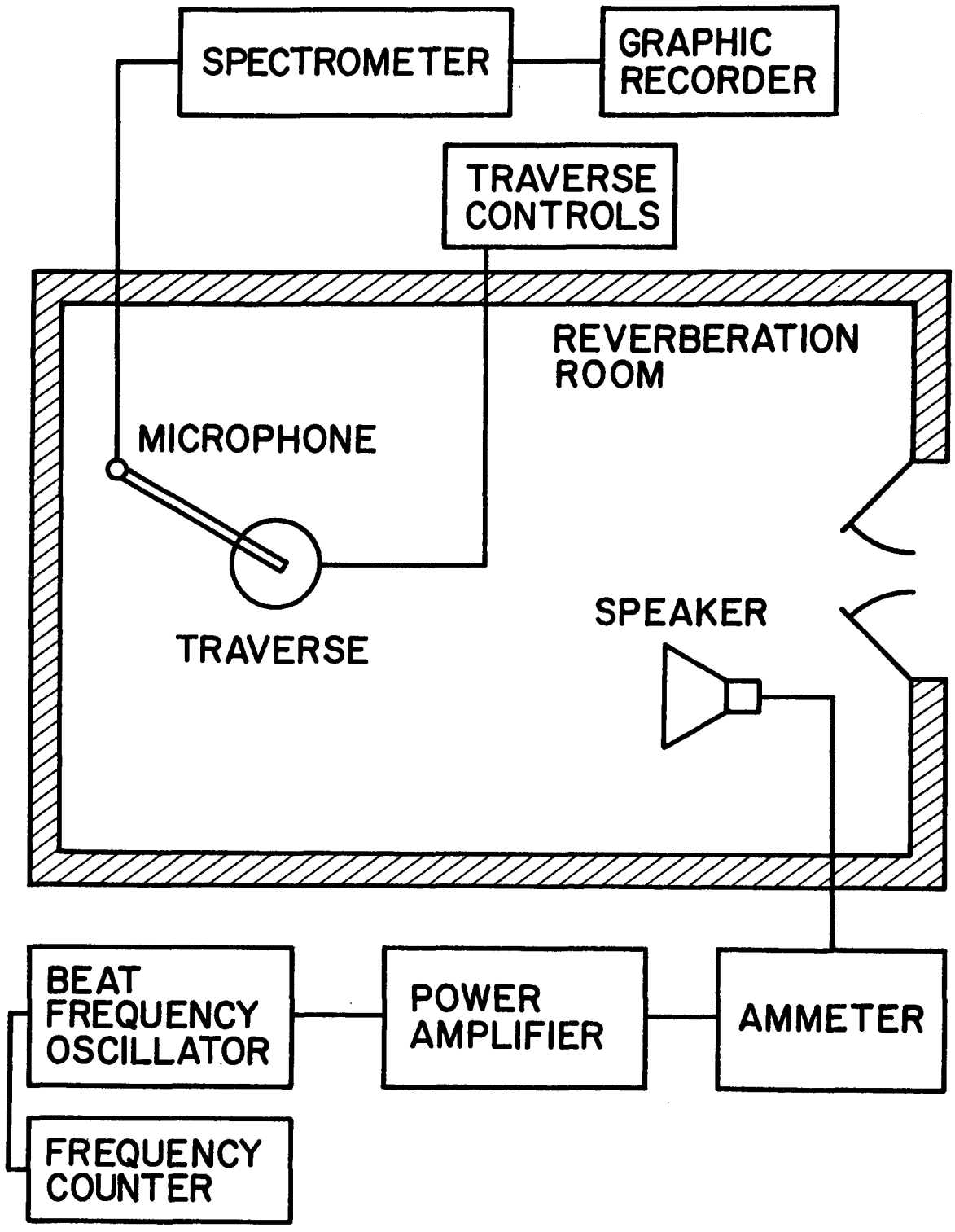

5.5 Experimental setup used to gather the statistical data

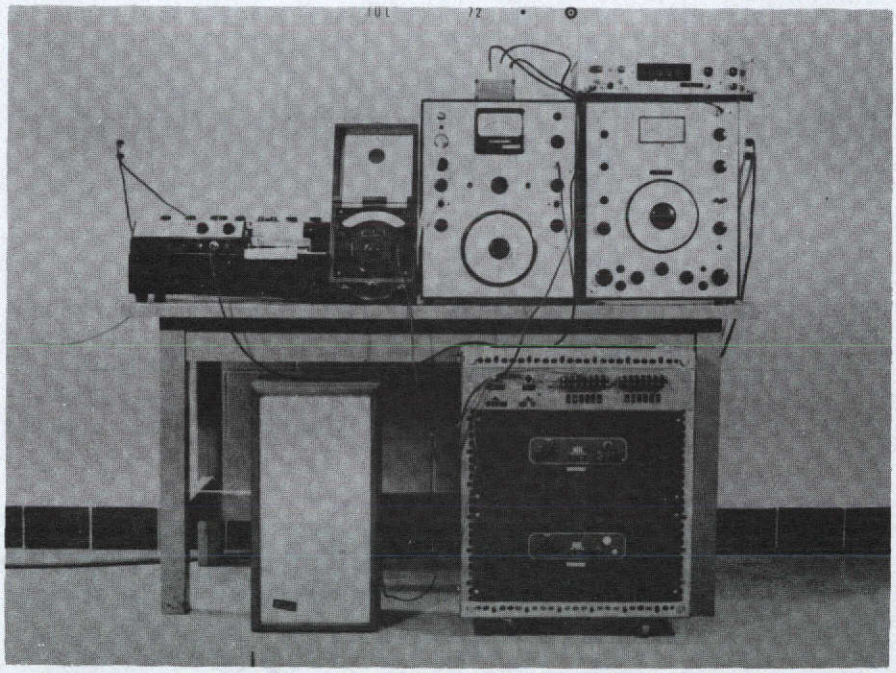

5.6 Photograph of the equipment setup used for data acquisition

5.2 Test Procedure

As was previously stated, the purpose of the experimental study was to obtain the data necessary to calculate the standard deviation of source power output from the mean output for low frequency, pure tone sound with source frequency, source size, and source location as the experimental parameters. As there is no instrument capable of measuring sound power directly, sound pressure must first be measured and then used to calculate the sound power. This relationship between sound pressure and sound power for any source located in a reverberant room is given by (4)

$$PWL = \overline{SPL} + 10 \log_{10} V - 10 \log_{10} T - 29.9 \quad , \tag{5.3}$$

where PWL = sound power level in dB, re 10^{-12} watts,

$\overline{SPL}$ = spatial average sound pressure level in dB, re 0.0002 μ bars,

V = room volume in ft^3,

T = reverberation time in sec.

Due to this proportionality of acoustic power to spatial average sound pressure, with all other quantities remaining constant for a given pure tone frequency, the variance associated with PWL is equal to that for $\overline{SPL}$. Thus, to eliminate the chore of calculating the power associated with each spatial average datum value, only the statistics of sound pressure are actually calculated in the remainder of this study.

It was decided to utilize four pure tone noise stimuli in the experimental study, namely 125 Hz, 250 Hz, 500 Hz, and 1000 Hz. It

should be noted that these selections correspond to the center frequencies of the third, fourth, and fifth standard octave bands, and, thus [from equation (3.6)], each successive frequency represents a fourfold increase in room modal density. The lowest excitation frequency, 125 Hz, was purposely chosen below the large room frequency of 134 Hz in order to test whether its corresponding statistics varied significantly from established theory for diffuse conditions.

Two sound sources were selected for use, one an eight inch diameter speaker and the other a 30 inch diameter speaker, in anticipation that a change would be seen in the power statistics due to the difference in finite source size. Since both the point source theory and the finite source theory are based on a monopole type source, these speakers were baffled to best model this monopole generation. A photograph of the two sources utilized is shown in Figure 5.7.

In selecting the source positions for use in this study, it was anticipated that only positions in which the speaker enclosure rested on the floor of the room would be utilized. In order for these source positions to be statistically independent, they had to be at least one-half a wavelength apart at the lowest frequency of interest. This, of course, amounted to 4.5 feet apart at 125 Hz. Also, due to the symmetry of the rectangular room, only source positions in one quadrant of floor area were considered. Using Beranek's (5) equation for the maximum number of source positions in a given space [modified slightly],

$$N \cong \frac{12Q}{\lambda^2} \quad , \tag{5.4}$$

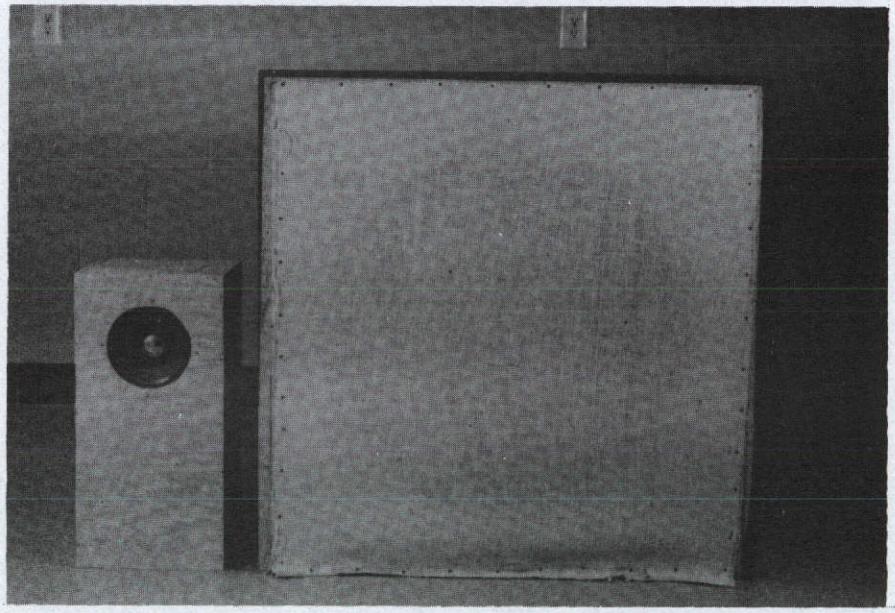

5.7 Photograph of the eight inch speaker and the 30 inch speaker used in the experimental study

where N = maximum number of independent source positions,

Q = area of floor quadrant,

λ = wavelength of lowest frequency,

it can be determined that a maximum of eleven positions is possible. Obviously, the larger the number of source positions, the higher will be the confidence in the resulting data. Thus, the maximum number of source positions was utilized, and they were arbitrarily selected as shown by the room quadrant layout in Figure 5.8.

In order to calculate the dependence of power statistics on source position for a given source, it is necessary to determine the spatial average sound pressure in the room for each source position. This spatial average is accomplished by measuring the sound pressure level at a number of independent locations in the sound field, i.e., at points at least one-half a wavelength apart, and then obtaining the logarithmic average of the resulting measurements. These microphone readings must be taken at a distance of at least one-half a wavelength from the source and at least one-fourth a wavelength from the room walls, since sound wave behavior in these areas deviates from the diffuse field condition. After careful consideration, it was decided that fifteen independent readings would provide a satisfactory approximation of the spatial average sound pressure level for each source position. The accuracy, of course, could have been improved with a larger number of microphone positions but the resulting increase in test effort by several orders of magnitude for just a small improvement in accuracy was not felt to be justifiable.

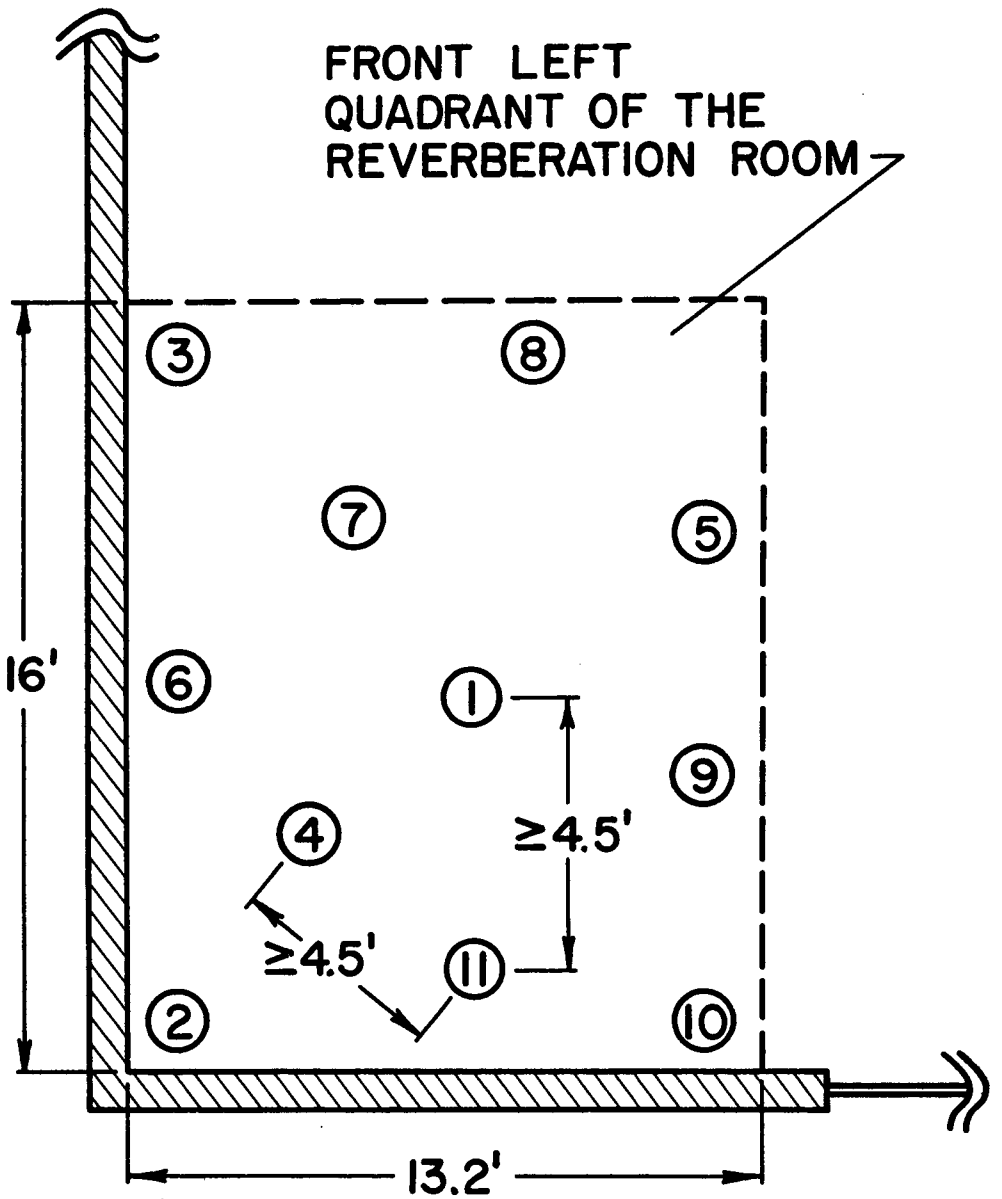

5.8 Approximate source positions used in the experimental study

The required microphone readings were obtained as discrete independent points using the microphone traverse. Even with the use of this device, however, quite a bit of work was involved in that several different traverses were necessary for each source position. Recall from Chapter 2 that Lubman's expression for the maximum number of readings from a circular arc traverse is

$$N = 1 + 2x/\lambda \quad , \tag{5.5}$$

where x is the traverse arc length. Using this relationship, the number of independent points for each frequency, given the traverse length to be 6.5 feet, is

125 Hz - 2 points/traverse,

250 Hz - 3 points/traverse,

500 Hz - 7 points/traverse,

1000 Hz - 12 points/traverse.

The required number of traverses can now be found by dividing the desired number of independent readings [namely 15] by each of the above relationships. The result is

125 Hz - 7.5 or 8 traverses , (5.6a)

250 Hz - 5 traverses , (5.6b)

500 Hz - 2.2 or 3 traverses , (5.6c)

1000 Hz - 1.3 or 2 traverses . (5.6d)

Two typical microphone traverse print-outs are shown in Figure 5.9. As is quickly noticed, fluctuations of 20 dB to 30 dB in the sound pressure level from point to point in the reverberant room are not uncommon.

The actual data gathering process consisted of making fifteen sound pressure level readings for each source at eleven source positions and at four excitation frequencies.[6] An attempt was made to regulate the speaker output in each test condition so that the average room sound pressure level was between 90 dB and 100 dB, a level at least 30 dB above the ambient noise.

The final result of this test operation was the compilation of 1155 data points, 660 points for the 30 inch speaker and 495 points for the eight inch speaker.

5.3 Data Analysis and Results

The compilation of experimental data is now analyzed using a standard two-way analysis of variance, namely an analysis both within and among source positions. This type of analysis can be facilitated by dividing the data into seven data point sets, with each set corresponding to a different combination of source size and excitation frequency. The result is 165 data points per set representing the different combinations of source position and microphone position. A typical data set, arranged in the form of a data point matrix, is shown in Table 5.3. Each element of the matrix y_{ij} represents the squared sound pressure for the ith source location as measured at the jth microphone position.

---

[6] Due to insufficient speaker output, no data was taken for the eight inch speaker at 125 Hz.

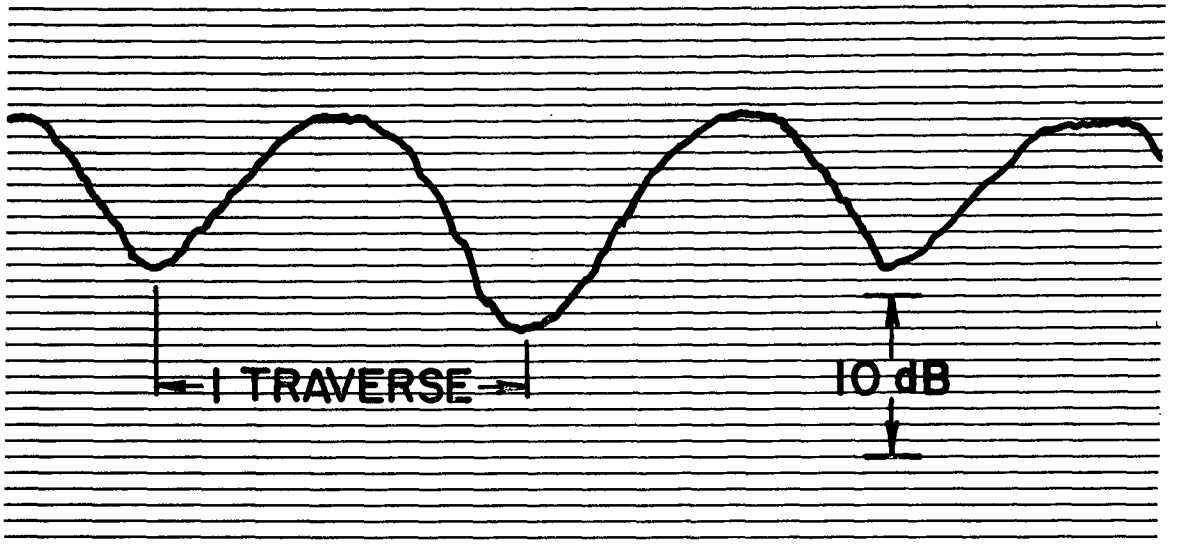

125 Hz

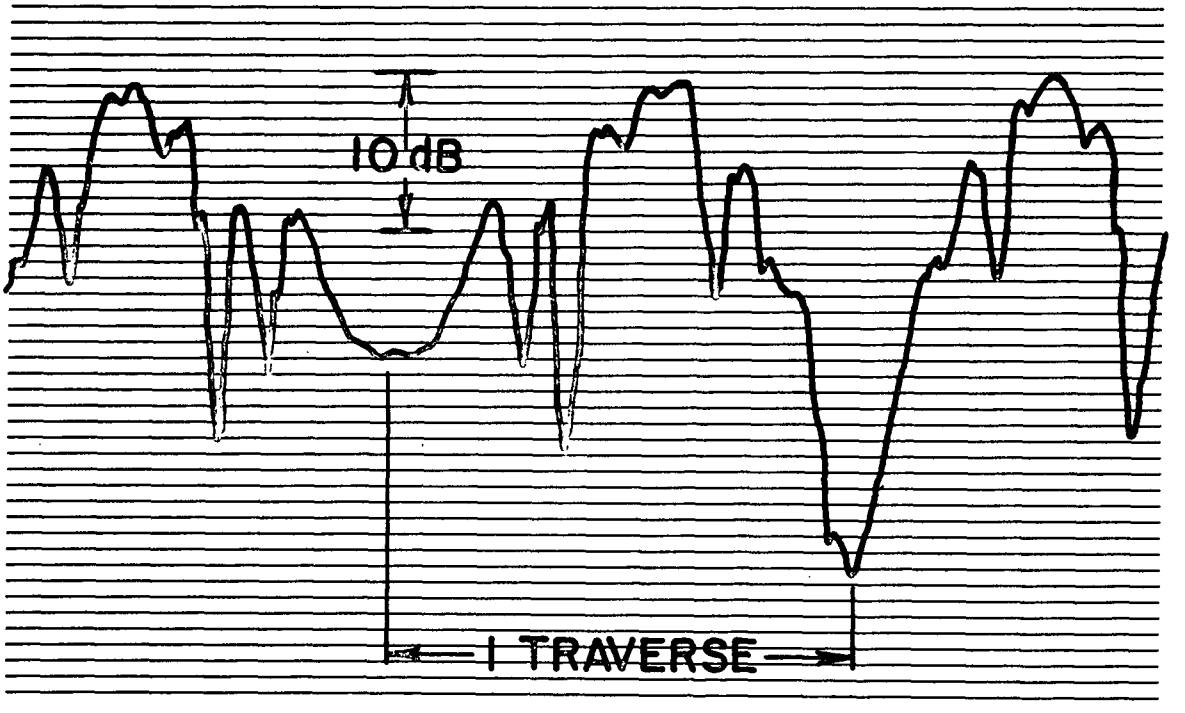

1000 Hz

5.9 Typical microphone traverse print-out data

Table 5.3 Data point matrix for a typical data set

Source Position	Microphone Position					
	1	2	3	4	. . .	n
1	y_{11}	y_{12}	y_{13}	y_{14}	. . .	y_{1n}
2	y_{21}	y_{22}	y_{23}	y_{24}	. . .	y_{2n}
3	y_{31}	y_{32}	y_{33}	y_{34}	. . .	y_{3n}
4	y_{41}	y_{42}	y_{43}	y_{44}	. . .	y_{4n}
.	.	.	.	.	.	.
..	.	.	.	.	. . .	.
.	.	.	.	.	.	.
s	y_{s1}	y_{s2}	y_{s3}	y_{s4}	. . .	y_{sn}

The symbol n represents the total number of microphone locations and s denotes the total number of source positions.

Utilizing Table 5.3, two new quantities can be defined which will prove very helpful in mathematically describing the analysis of variance technique. These quantities are the spatial average sound pressure in the room for the source at the ith position, given by

$$P_i = \sum_{j=1}^{n} \frac{y_{ij}}{n} \quad , \tag{5.7}$$

and the mean value of the spatial average pressures for all i source positions, given by

$$G = \sum_{i=1}^{s} \frac{P_i}{S} \quad . \tag{5.8}$$

Consideration is first given to the average value of the normalized variance <u>within</u> source positions for a given data set. Based on a single microphone reading for each source position, this average variance can be expressed mathematically as

$$\sigma_A^2 = \frac{1}{S} \sum_{i=1}^{s} \frac{1}{n-1} \sum_{j=1}^{n} \frac{(y_{ij}-P_i)^2}{P_i^2} \quad . \tag{5.9}$$

This equation, which is applied to each data set, states, first of all, that the spatial average sound pressure in the room P_i is calculated for the ith position of the source. The spatial average is then subtracted from each of the individual microphone readings y_{ij} for that source position, and each result is then squared. The sum of these

squares over all n microphone positions, followed by division by $P_i^2(n-1)$, gives the normalized variance of a single microphone reading from the mean for the ith source position. If the above calculation is performed for all i source positions, and if the resulting variances are averaged, then the average normalized variance σ_A^2 of sound pressure for a single microphone reading is obtained for that data set. A calculation of this type is presented in Appendix 9.3 using an actual data set obtained from experimental investigation.

The results of this analysis within source positions are given in Table 5.4 for each frequency and source size. It can be seen that both the variance and the standard deviation of the data are presented in both normalized form and in decibels. As to whether the normalized standard deviation or the standard deviation in decibels is more useful depends entirely upon the particular application. Thus, it is extremely helpful to be able to quickly find one form of the standard deviation given the other form. A graph showing the relationship between the two forms is given in Figure 5.10.

It should be kept in mind that the results in Table 5.4 are based on a single microphone reading. As was mentioned in Chapter 2, if the spatial average sound pressure is based upon n microphone readings, the normalized variance is reduced by a factor of 1/n or

$$\sigma_B^2 = \sigma_A^2/n \quad , \tag{5.10}$$

Table 5.4 Experimental uncertainty of pure tone mean square sound pressure using a single microphone position

Source Size (in)	Frequency (Hz)	Variance (dB)	Standard Deviation (dB)	Variance (normal)	Standard Deviation (normal)
8	250	33.99	5.83	1.06	1.03
	500	37.09	6.09	1.12	1.06
	1000	35.52	5.96	1.08	1.04
30	125	28.20	5.31	0.92	0.96
	250	36.48	6.04	1.10	1.05
	500	35.40	5.95	1.08	1.04
	1000	28.41	5.33	0.92	0.96

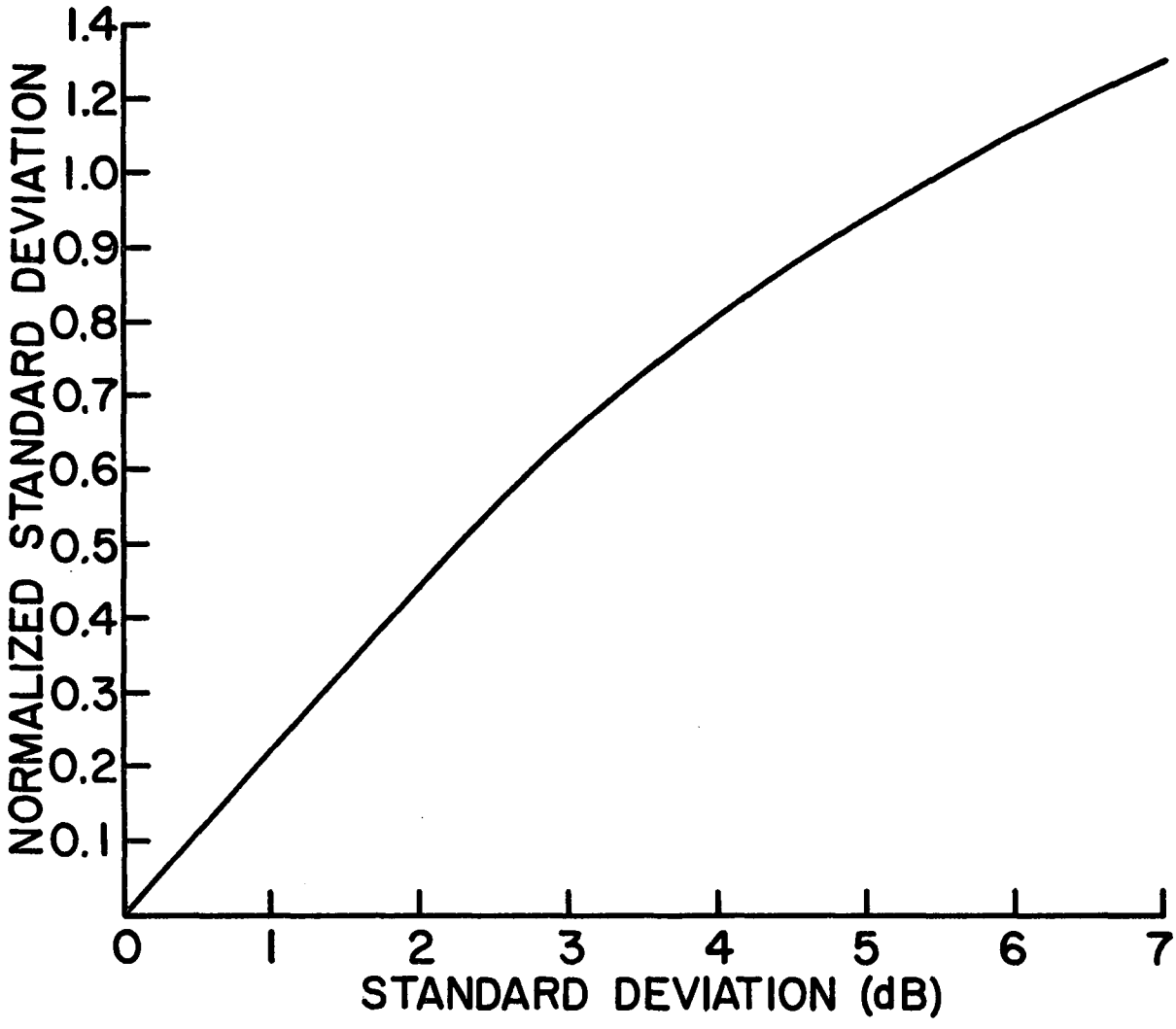

5.10 Graph for converting normalized standard deviation to standard deviation in decibels

where σ_B^2 = normalized variance due to a spatial average based on n microphone readings,

σ_A^2 = normalized variance due to a spatial average based on one microphone reading.

The second part of the analysis of variance is performed to find the total variance or the variance among source positions. Based on n microphone positions per source position, this normalized variance of spatial average sound pressure [or sound power] from the mean pressure [or power] for all s source positions can be expressed mathematically using Table 5.3, equation (5.7), and equation (5.8). The result is

$$\sigma_C^2 = \frac{1}{S-1} \sum_{i=1}^{s} \frac{(P_i - G)^2}{G^2} \quad . \tag{5.11}$$

The mathematical operations involved in equation (5.11) are, first of all, the determination of the mean value G of the spatial average pressures in the room for all s source positions. This mean value is then subtracted in turn from each of the spatial average pressures P_i. Each resultant is then squared, and a sum is taken over all s squares. After division by $G^2(S-1)$, this sum represents the total normalized variance of source power from the mean based on the fact that the spatial average room pressure for each source position was determined using n microphone locations.

As should be expected, therefore, the normalized variance given by equation (5.11) is actually the sum of two independent variances. One

variance is that due to incomplete spatial averaging of the resultant sound field for each source position. The value of this variance has already been determined and is given by equation (5.10). The second variance is that due to changes in source power caused by variations in source position. In other words,

$$\sigma_C^2 = \sigma_B^2 + \sigma_N^2 \quad , \tag{5.12}$$

where σ_N^2 is the normalized variance due solely to changes in source position. The significance of this relationship may not be evident at this time, however in Chapter 6, where a comparison is made between theory and experiment, its utilization will be essential.

A sample calculation of the total variance using an actual data set is given in Appendix 9.4. It should be emphasized again that the actual quantity determined in the Appendix is the variance of mean square pressure. However, due to the proportionality of mean square sound pressure to sound power, the quantity also represents the variance of sound power.

The results of the statistical analysis of variance among source positions are given in Table 5.5. Again both the variance and standard deviation of each data set are presented in both normalized form and in decibels.

Table 5.5 Experimental uncertainty of pure tone sound power using a single source position

Source Size (in)	Frequency (Hz)	Variance (dB)	Standard Deviation (dB)	Variance (normal)	Standard Deviation (normal)
8	250	3.50	1.87	0.172	0.415
	500	2.82	1.68	0.137	0.370
	1000	1.39	1.18	0.072	0.268
30	125	5.38	2.32	0.260	0.510
	250	0.92	0.96	0.048	0.219
	500	1.46	1.21	0.073	0.271
	1000	1.61	1.27	0.081	0.284

6. COMPARISON OF THEORY AND EXPERIMENT

Since the experimental results were presented in two parts - the variance within source positions and the variance among source positions, the comparison between theory and experiment will be presented in the same way.

First consider the standard deviation of spatial average pressure within source positions for each data set. Recall from Chapter 2 that Doak in 1959 and Lubman in 1968 showed theoretically that this standard deviation for a pure tone source should equal 5.57 dB or, when normalized, should equal one. Comparing these theoretical findings to the experimental results of Table 5.4, the plots shown in Figure 6.1 for the eight inch speaker and in Figure 6.2 for the 30 inch speaker are obtained. For both source sizes, the agreement between theory and experiment is quite good.

In order to test the hypothesis that the true finite source standard deviation is equal to the theoretical value of one, a chi-squared, χ^2, distribution is assumed (10). A test using such a distribution involves the definition of a new variable given by

$$v = \frac{(n-1)S^2}{\sigma^2} \quad , \tag{6.1}$$

where v = experimental variable,

$(n-1)$ = degrees of freedom,

S = experimentally determined normalized standard deviation,

σ = true standard deviation of the finite source.

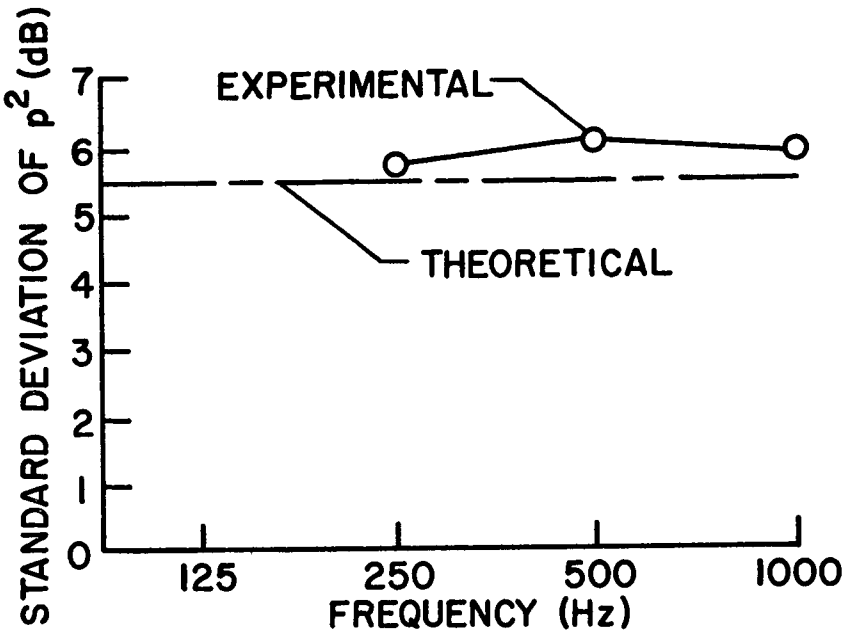

6.1 Uncertainty of pure tone sound pressure from an eight inch speaker using a single microphone position

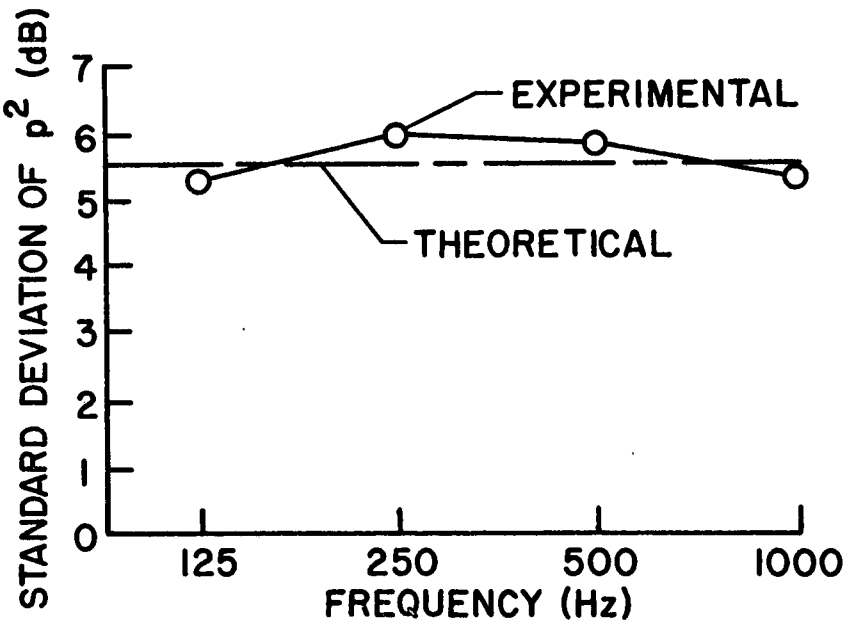

6.2 Uncertainty of pure tone sound pressure from a 30 inch speaker using a single microphone position

For this case, the variable v possesses a χ^2 distribution with 164 degrees of freedom. If χ_1^2 and χ_2^2 represent the two values of χ^2 cutting off Z per cent tail areas, then the probability is (100 - 2Z) per cent that v will satisfy

$$\chi_1^2 < v < \chi_2^2 \quad . \tag{6.2}$$

Substituting equation (6.1) into equation (6.2), followed by algebraic manipulation, yields

$$\frac{(n-1)S^2}{\chi_2^2} < \sigma^2 < \frac{(n-1)S^2}{\chi_1^2} \quad . \tag{6.3}$$

This expression is known as the Z per cent confidence interval for σ^2. Taking the worst experimental case, namely S = 1.06 for the eight inch speaker at 500 Hz, the confidence interval becomes

$$\frac{183.5}{\chi_2^2} < \sigma^2 < \frac{183.5}{\chi_1^2} \quad . \tag{6.4}$$

Arbitrarily choosing a confidence level of 95 per cent, the χ^2 tables indicate

$$\chi_1^2 = 129.98 \quad , \tag{6.5a}$$

$$\chi_2^2 = 200.86 \quad . \tag{6.5b}$$

Substitution of equations (6.5a) and (6.5b) into equation (6.4), followed by the square root, yields

$$0.96 < \sigma < 1.19 \tag{6.6}$$

for the 95 per cent confidence interval for the true finite source standard deviation [using the worst experimental case]. This interval includes the theoretical value of one, and, therefore the hypothesis is accepted with at least 95 per cent certainty.

Secondly, the standard deviation of source power among source positions is considered. The normalized standard deviations of this type for a point source are determined theoretically using equation (3.9). With a room volume of 8000 ft^3, this equation becomes

$$\sigma_{N(P.S.)} = 3.69 \times 10^2 \frac{T}{f}^{1/2} , \qquad (6.7)$$

where the reverberation times are given in Table 5.2 for each frequency f.

The theoretical standard deviations for both finite source sizes are then found using equation (4.45). The values of $(2\xi/\pi)^{1/2}$ needed to evaluate this equation can be read from Figure 4.5, in which

$$kd \text{ (30 inch speaker)} = 1.40 \times 10^{-2} f ,$$

$$kd \text{ (8 inch speaker)} = 3.75 \times 10^{-3} f .$$

The theoretical standard deviations determined for a point source and for the finite sources, however, are made assuming that the spatial average pressure in the room is known exactly for each possible source position. In other words, the theoretical values do not account for the incomplete spatial averaging inherent in the experimental results. Thus, before any comparison between theory and experiment can be attempted, the theoretical values must be adjusted to account for this extra experimental error. The required additive standard deviation due

to incomplete averaging can be found from equation (5.10) to be

$$\sigma_B = (1/15)^{1/2} = 0.258 \quad , \tag{6.8}$$

or about 1.1 dB. Substitution of the theoretical values of $\sigma_{N\,(P.S.)}^2$ and $\sigma_{N\,(F.S.)}^2$ and the value of σ_B from equation (6.8) into equation (5.12) then gives the adjusted theoretical values appropriate for comparison with experimental results.

The theoretical results for the two finite sources and for a point source are given in Table 6.1. This table includes both the adjusted and unadjusted values of standard deviation. [Recall that the experimental results for both finite sources was given in Table 5.5].

Figure 6.3 is a graph comparing the experimental and the adjusted theoretical results for the eight inch speaker to that predicted by point source theory. In addition to showing good agreement between finite source theory and experiment, both curves also fall near point source predictions. This should not be surprising due to the small value of kd for the eight inch speaker at low frequencies.

The results for the 30 inch speaker are shown in Figure 6.4. Again, the agreement between the experimental results and the derived finite source theory is good. However, both finite source curves fall measurably below the standard deviations predicted by point source theory, especially at the two lower frequencies. The lack of a dramatic decrease at the two higher frequencies is due, at least in part, to the fact that the standard deviation attributable to incomplete spatial averaging [indicated by the dashed horizontal line in the figure] has become the dominant term in the total uncertainty.

Table 6.1 Theoretical uncertainty of pure tone sound power using a single source position (adjusted values are those including the error due to experimental incomplete spatial averaging)

Source Size (in)	Frequency (Hz)	Standard Deviation (dB)	Adjusted Standard Deviation (dB)	Standard Deviation (normal)	Adjusted Standard Deviation (normal)
point	125	3.17	3.50	0.673	0.720
	250	1.53	1.93	0.337	0.424
	500	0.67	1.35	0.152	0.300
	1000	0.37	1.20	0.073	0.268
8	125	3.10	3.43	0.664	0.712
	250	1.45	1.87	0.320	0.411
	500	0.52	1.28	0.124	0.286
	1000	0.10	1.15	0.030	0.286
30	125	2.57	2.85	0.565	0.621
	250	0.67	1.35	0.155	0.300
	500	0.12	1.15	0.032	0.260
	1000	0.05	1.13	0.002	0.258

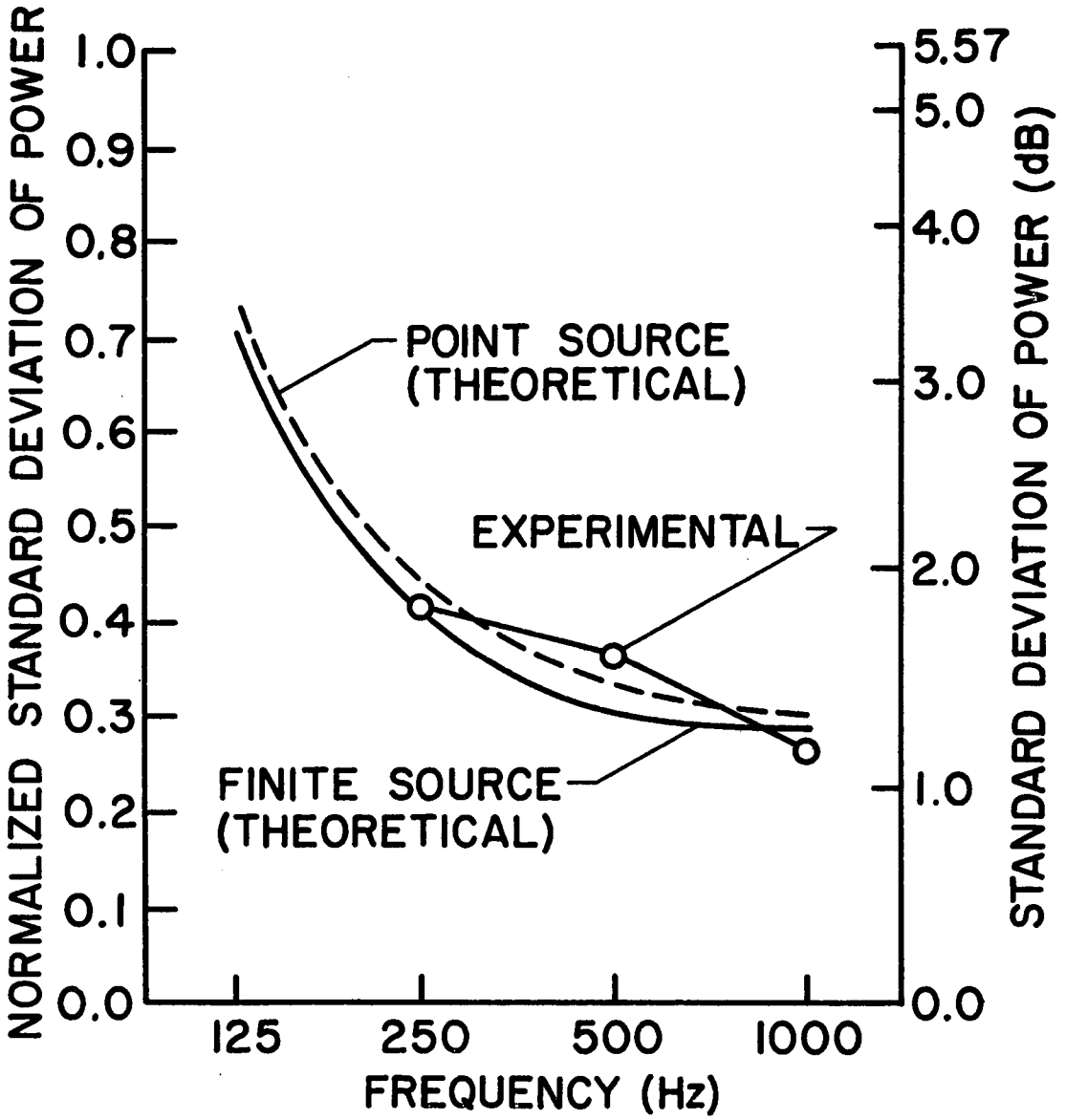

6.3 Uncertainty of pure tone sound power from an eight inch speaker using a single source position

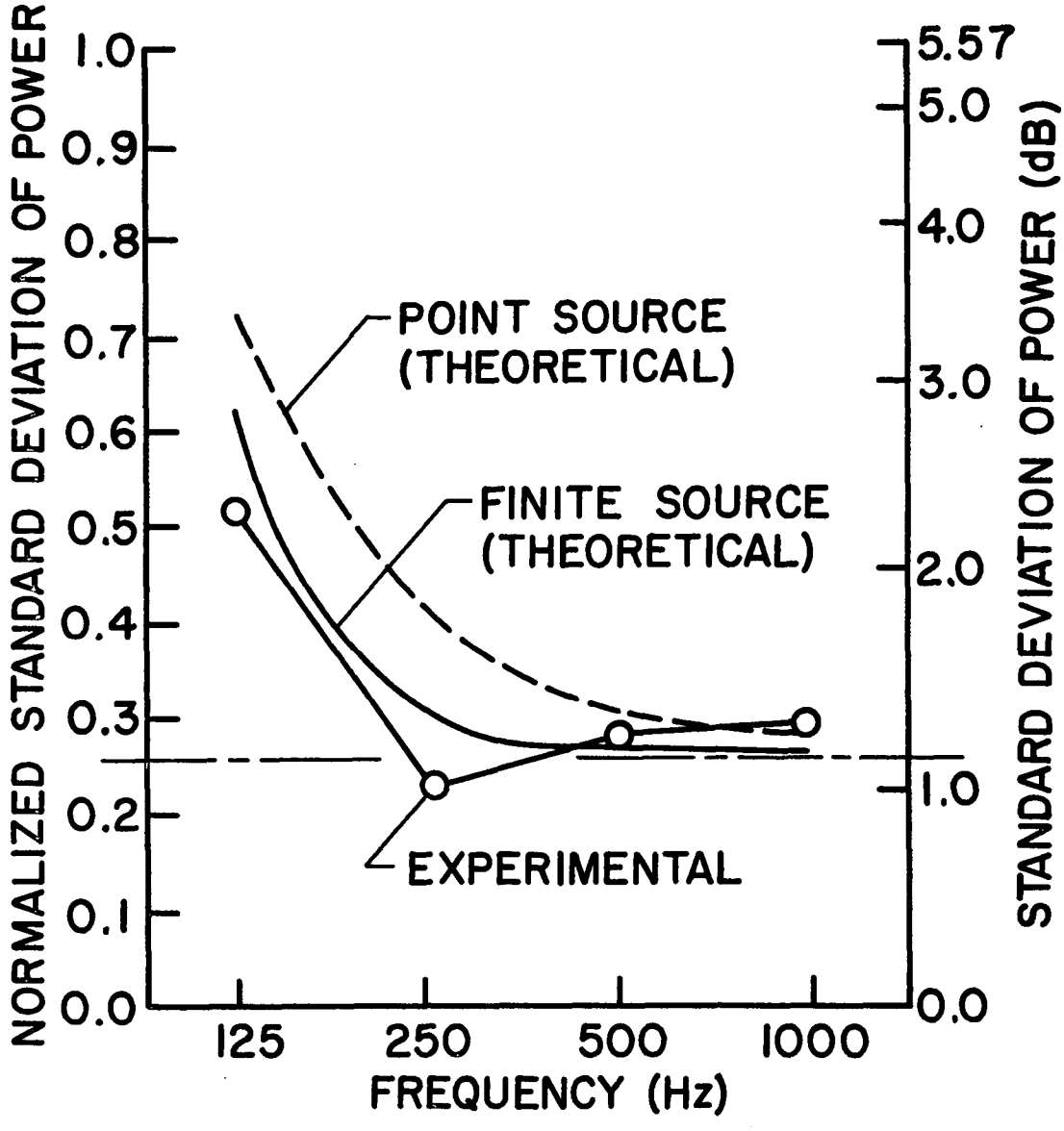

6.4 Uncertainty of pure tone sound power from a 30 inch speaker using a single source position

Due to the limited number of source positions utilized in this study, it is important to determine the confidence which can be associated with the conclusion that the standard deviation for the 30 inch speaker is less than that for a point source. If a χ^2 distribution is again assumed with the variable v defined by equation (6.1), then the probability is (100 - Z) per cent that v will satisfy

$$v < \chi_1^2 \quad , \tag{6.9}$$

where χ_1^2 is the value of χ^2 cutting off a Z per cent lower tail area. In other words, the upper confidence limit cutoff value for the true variance of the finite source data is

$$\sigma^2 < \frac{(n-1)S^2}{\chi_1^2} \quad . \tag{6.10}$$

Taking the data point at 125 Hz where S = 0.621 as a typical value, then equation (6.10) with n = 11 source positions yields

$$\sigma^2 < \frac{3.84}{\chi_1^2} \quad . \tag{6.11}$$

Assuming a confidence level of 70 per cent which corresponds to

$$\chi_1^2 = 7.50 \quad ,$$

equation (6.11) yields

$$\sigma < 0.715 \quad . \tag{6.12}$$

This upper limiting value is less than the standard deviation of 0.720 predicted by point theory. Therefore, since the confidence level associated with the 250 Hz point is much greater than 70 per cent, it may be stated with at least 70 per cent confidence that the standard deviation of power for the 30 inch speaker at 125 Hz and at 250 Hz is less than that predicted by point source theory. Unfortunately, the dominance of the uncertainty due to incomplete spatial averaging at 500 Hz and 1000 Hz prevents the establishment of any meaningful conclusions from the experimental results at these frequencies. As previously stated in Section 5.2, the uncertainty due to incomplete spatial averaging could have been decreased with a larger number of microphone readings, but the huge increase in test effort necessary for a small increase in accuracy was not felt to be justified.

7. SUMMARY AND CONCLUSIONS

Three significant conclusions can be drawn from the results of this study. First of all, if two monopole type sources, one a point source and the other the finite source model, have equal volume velocities, their diffuse field acoustic power output is also the same. Furthermore, the diffuse field power outputs for both source sizes are equal to the corresponding powers as measured in the free field.

Secondly, for a finite source, the standard deviation from the mean of pure tone sound pressure at a point is equal to that derived for any pure tone source located at some given source position. Furthermore, this standard deviation is independent of source size or source frequency and has a decibel value of 5.57 dB or a normalized value of one.

Finally, the normalized standard deviation of low frequency, pure tone sound power output for a monopole type finite size source is lower than that predicted for a point source. This decrease is considerable when the ratio of source dimension to acoustic wavelength is one-half or greater. The significance of this conclusion is that in some cases the reliable measurement of sound power output (within about $\pm$ 2 dB) of a low frequency, pure tone finite size source can be made without utilizing the large number of source positions required by point source theory. In other words, the use of a reverberation room to measure the power output of a finite size source, even for source spectrums containing a large, low frequency pure tone or narrow-band component, may prove to be quite attractive. This should especially prove to be true for

rooms equipped with rotating diffusers which decrease the sound pressure fluctuations caused by the room modes.

In addition to the above conclusions, another contribution of this study is the development of a microphone traversing apparatus to facilitate the determination of spatial average pressure. This traversing device was used extensively in this study and could prove quite useful in future reverberant field research studies at the Center for Acoustical Studies. To the author's knowledge, such a traversing mechanism is not available in the commercial market.

While this study has provided understanding of one of the important missing links in the use of reverberant rooms for sound power measurements, additional extensive research is needed before a satisfactory "total" understanding is achieved. For example, the work done in this study and the majority of work done concerning point sources has been established assuming the source to have monopole type radiation characteristics. The statistics of sources having dipole, quadrapole, and higher order characteristics are essentially unknown. However, two research projects concentrating on dipole behavior are presently underway. Although the results are not yet available, Yousri and Fahy at the University of Southampton are studying the statistics of point dipole sources in reverberant rooms. In another effort, Lubman is studying the behavior of the ILG or "random dipole" source. Although once again the results are not yet available, the claims that preliminary indications show a higher standard deviation than for a point monopole source, at least at low frequencies. Both of these research efforts should provide still another stepping stone toward the establishment of a high level of confidence in reverberant room measurements.

In addition, as far as finite size sources are concerned, this study investigated only one type of source orientation - that parallel to the y-z plane. The statistics of other orientations, such as a skew orientation, have not been investigated. Finally, Eldred[7] has suggested that the modal density of reverberant rooms excited by large sources might be decreased by several orders of magnitude at high frequencies due to poor coupling between the source and the sound field. Although this theory has not been fully substantiated, it could foreseeably add another factor of confusion into the many problems already known.

However, even with the present existing problems, it would appear that in the near future the reverberant room may emerge as the most extensively utilized device for any type of acoustical measurement not requiring directivity information.

---

[7] The concept of decreased modal density was brought out in "Effective Modal Density in a Reverberant Sound Field for Finite Sized Sources" by B. H. Sharp and K. M. Eldrea, presented to the Acoustical Society of America, April 18, 1972.

8. LIST OF REFERENCES

1. American Society of Heating, Refrigerating, and Air Conditioning Engineers. 1962. Measurement of sound power radiated from heating, refrigeration, and air conditioning equipment. ASHRAE 36-62.

2. Baade, P. K. 1971. Equipment sound power measurements in reverberation rooms. J. Sound Vibr. 16(1):131-135.

3. Beranek, L. L. 1954. Acoustics. McGraw-Hill Book Company, New York.

4. Beranek, LL. 1960. Noise Reduction. McGraw-Hill Book Company, New York.

5. Beranek, L. L. 1971. Noise and Vibration Control. McGraw-Hill Book Company, New York.

6. Bolt, R. H. and R. W. Roop. 1950. Frequency response fluctuations in rooms. J. Acoust. Soc. Amer. 22(2):280-289.

7. Doak, P. E. 1959. Fluctuations of the sound pressure level in rooms when the receiver position is varied. Acustica 9(1): 1-9.

8. Dodd, S. D. and P. E. Doak. 1971. Some aspects of the theory of diffusion and diffusers. J. Sound Vibr. 16(1):89-98.

9. Ebbing, C. E. 1969. Experimental evaluation of moving sound diffusers for reverberant rooms. J. Sound Vibr. 16(1):99-118.

10. Hoel, P. G. 1966. Elementary Statistics. John Wiley and Sons, Inc., New York.

11. Kinsler, L. E. and A. R. Frey. 1962. Fundamentals of Acoustics. John Wiley and Sons, Inc., New York.

12. Lubman, D. 1968. Fluctuation of sound with position in a reverberant room. J. Acoust. Soc. Amer. 44(6):1491-1502.

13. Lubman, D. 1969. Spatial averaging in a diffuse sound field. J. Acoust. Soc. Amer. 46(3):532-534.

14. Lyon, R. H. 1969. Statistical analysis of power injection and response in structures and rooms. J. Acoust. Soc. Amer. 45(3):545-565.

LIST OF REFERENCES (continued)

15. Maling, G. C. 1967. Calculation of the acoustic power radiated by a monopole in a reverberation chamber. J. Acoust. Soc. Amer. 42(4):859-865.

16. Morse, P. M. 1948. Vibration and Sound. McGraw-Hill Book Company, New York.

17. Morse, P. M. and K. U. Ingard. 1968. Theoretical Acoustics. McGraw-Hill Book Company, New York.

18. Rice, S. O. 1951. Mathematical analysis of random noise. A contribution to Noise and Stochastic Processes, Nelson Wax, Editor. Dover Publications, Inc., New York, Sec. 1.5:153.

19. Sabine, W. C. 1964. Reverberation. A contribution to Collected Papers on Acoustics. Dover Publications, Inc., New York.

20. Schroeder, M. R. 1962. Frequency-correlation functions of frequency responses in rooms. J. Acoust. Soc. Amer. 34(12): 1819-1823.

21. Schultz, T. J. 1971. Diffusion in reverberation rooms. J. Sound Vibr. 16(1):17-28.

22. Schultz, T. J. 1971. Sound power measurements in a reverberant room. J. Sound Vibr. 16(1):119-129.

23. Sepmeyer, L. W. 1965. Computed frequency and angular distribution of normal modes of vibration in rectangular rooms. J. Acoust. Soc. Amer. 37(2):413-423.

24. Seto, W. W. 1971. Acoustics. McGraw-Hill Book Company, New York.

25. United States Department of Labor. 1971. Guidelines to the Department of Labor's occupational noise standard. Bulletin 334, Washington, D. C.

26. Waterhouse, R. V. 1968. Statistical properties of reverberant sound fields. J. Acoust. Soc. Amer. 43(6):1436-1444.

9. APPENDICES

9.1 Numerical Integration Procedure

The objective of the numerical integration procedure is to obtain good approximations for equation (4.24) and for equation (4.28) as a function of the quantity $k_m d$. Due to the similarity of these two equations, the same numerical procedure is utilized to integrate both expressions. Therefore, the actual computer programs are essentially alike for both approximations, except for the obvious difference in the two integrands.

The procedure developed consists of approximating each integral as a finite double sum over θ and γ with the limits for both sums being from zero to $\pi/2$. The accuracy of each approximation is controlled by the number of point values included within each summing interval.

For simplicity in describing the computer programs, let k represent both $\langle\phi^2\rangle \sin\theta$ in equation (4.24) and $\langle\phi^4\rangle \sin\theta$ in equation (4.28), where it is understood that k is a function of θ, γ, and $k_m d$ for both cases. A conventional digital computer flow diagram can then be used to describe the basic steps in the numerical procedure. This flow diagram is shown in Figure 9.1.

9.2 Microphone Traverse

Even before this study was undertaken, it was determined that a microphone traverse mechanism was needed to facilitate the determination of spatial average pressure in the reverberation room. It was intended that this device would move a microphone either through a straight line

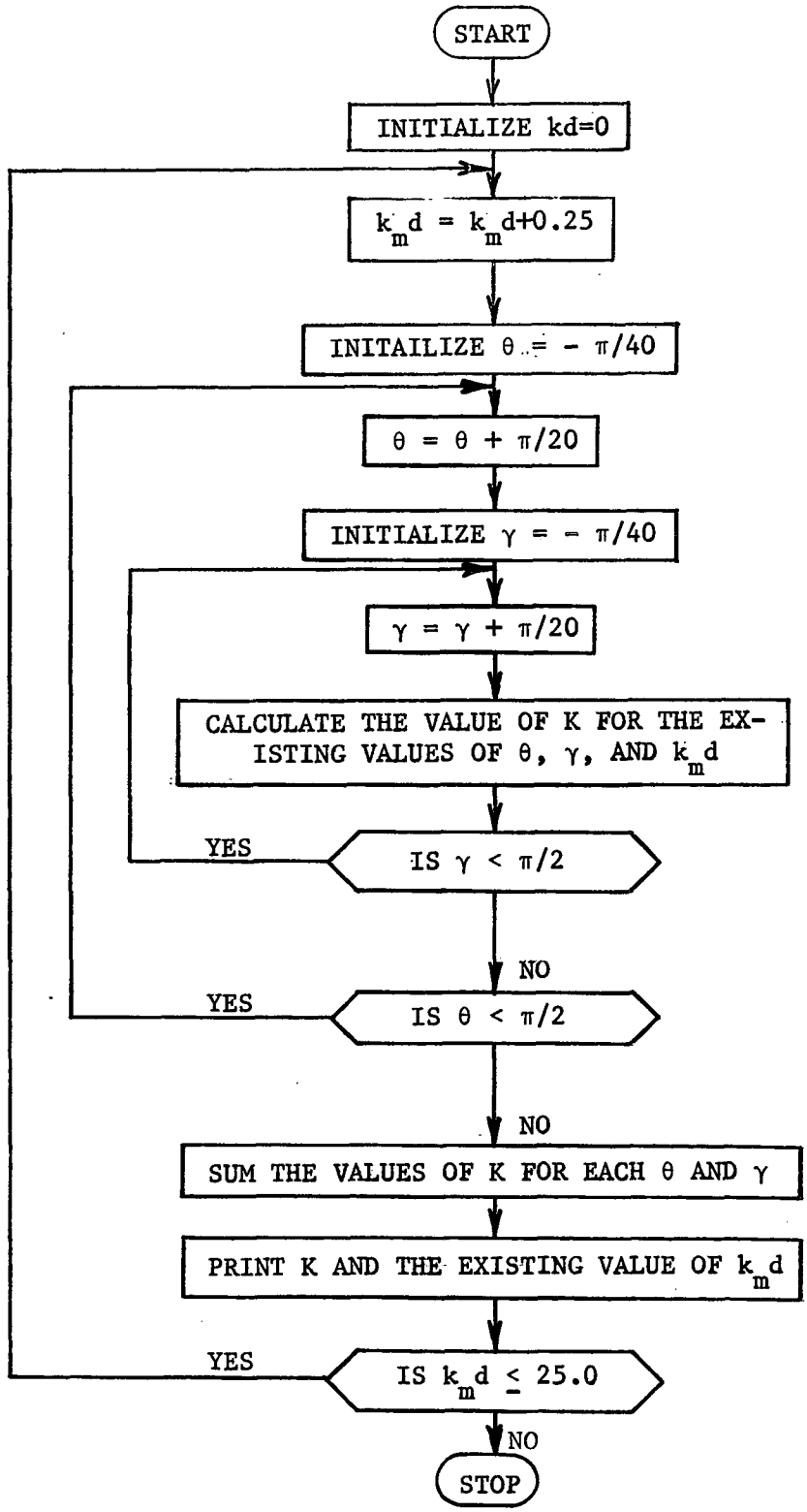

Figure 9.1. Flow diagram of the numerical integration program.

or through a circular arc, and thus provide several independent pressure readings at one time.

In the preliminary stages of design, several criteria were established to ensure that the device would meet expectations. First of all, the need for a means of adjusting the traverse length was felt to be desirable. The use of this device in different sized rooms and for different frequency ranges might warrant such an adjustment. Secondly, the traverse had to make a minimum of noise during operation. Any operational noise could interfere with the acoustical signal being detected. This criterion placed quite a restriction on the design, since it practically prohibited the use of any motorized device. Next, the device was to be controllable from outside the reverberation room. It was intended that this stipulation would prevent any operator disturbance of the sound field by enabling the operator to start and stop the device at will without having to enter the reverberation facility. It was also felt that the microphone motion itself should be as constant as possible so that repeated tests under the same conditions would produce the same data print-outs. Next, economic factors had to be considered, since funds were not available for a large expenditure. The design had to be geared toward construction using existing materials or ones which were inexpensive and readily available. Finally, the traverse had to be durable enough to withstand continual movement from one room location to another and yet be light enough to facilitate relocations without much effort.

Before attempting to completely design such a device, a search was made to see if a device meeting these specifications already existed at

any of the well known research centers in the country. One such center claimed to have such a device, and, therefore, a complete set of working drawings was purchased from them. These plans were quite helpful in providing a good design basis, but as far as a practical and usable final design was concerned, the plans were rather incomplete and the finished produce highly unacceptable. Many design alterations were made before an acceptable traversing apparatus was obtained.

While the original plans called for a hydraulic device actuated by pressurized air, the device actually constructed operates entirely on pressurized air. Boom vertical motion is produced by the continuous compression and decompression of a standard type air cylinder. Control of the motion is accomplished using mercury switches on the traverse boom and an electrical relay in the control box which actuates the air inlet and exhaust valves. Since both of the valves and the relay are located outside the test room, the only noise produced by the traverse mechanism itself is the frictional noise of the air cylinder piston and of the boom bearing.

The length of the boom itself provides the necessary control over the microphone sweep length. Furthermore, this boom as well as the majority of the device, is constructed of aluminum, thereby limiting the total weight to about twenty pounds. Most of this weight is attributable to two inertial masses located on the boom which serve to provide smooth motion at a moderate angular velocity.

Figure 9.2 shows a simplified drawing of the basic components of the microphone traverse device. This is followed in Figure 9.3 by a drawing of the unit designed to control the traverse motion.

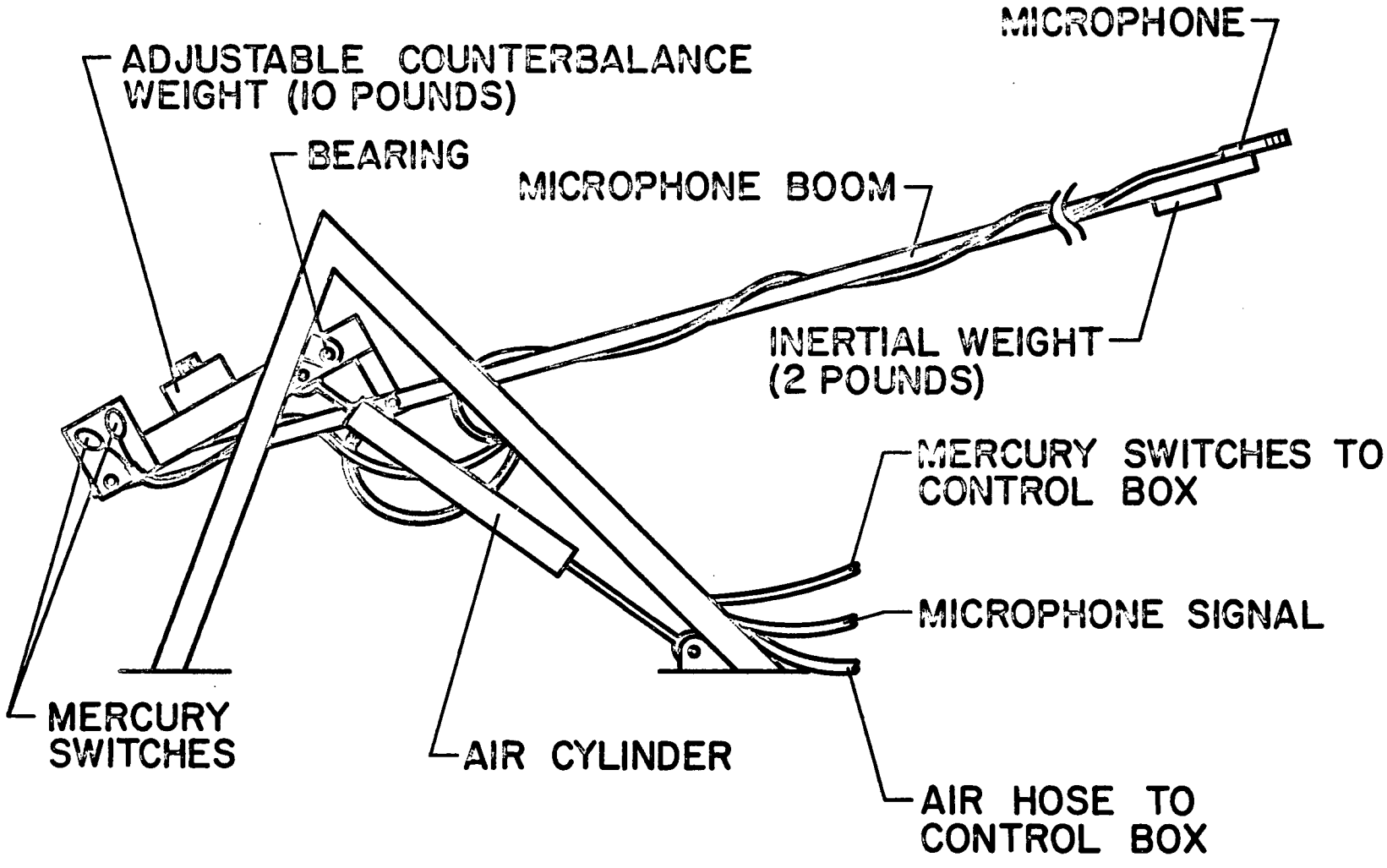

9.2 Simplified drawing of the microphone traverse apparatus

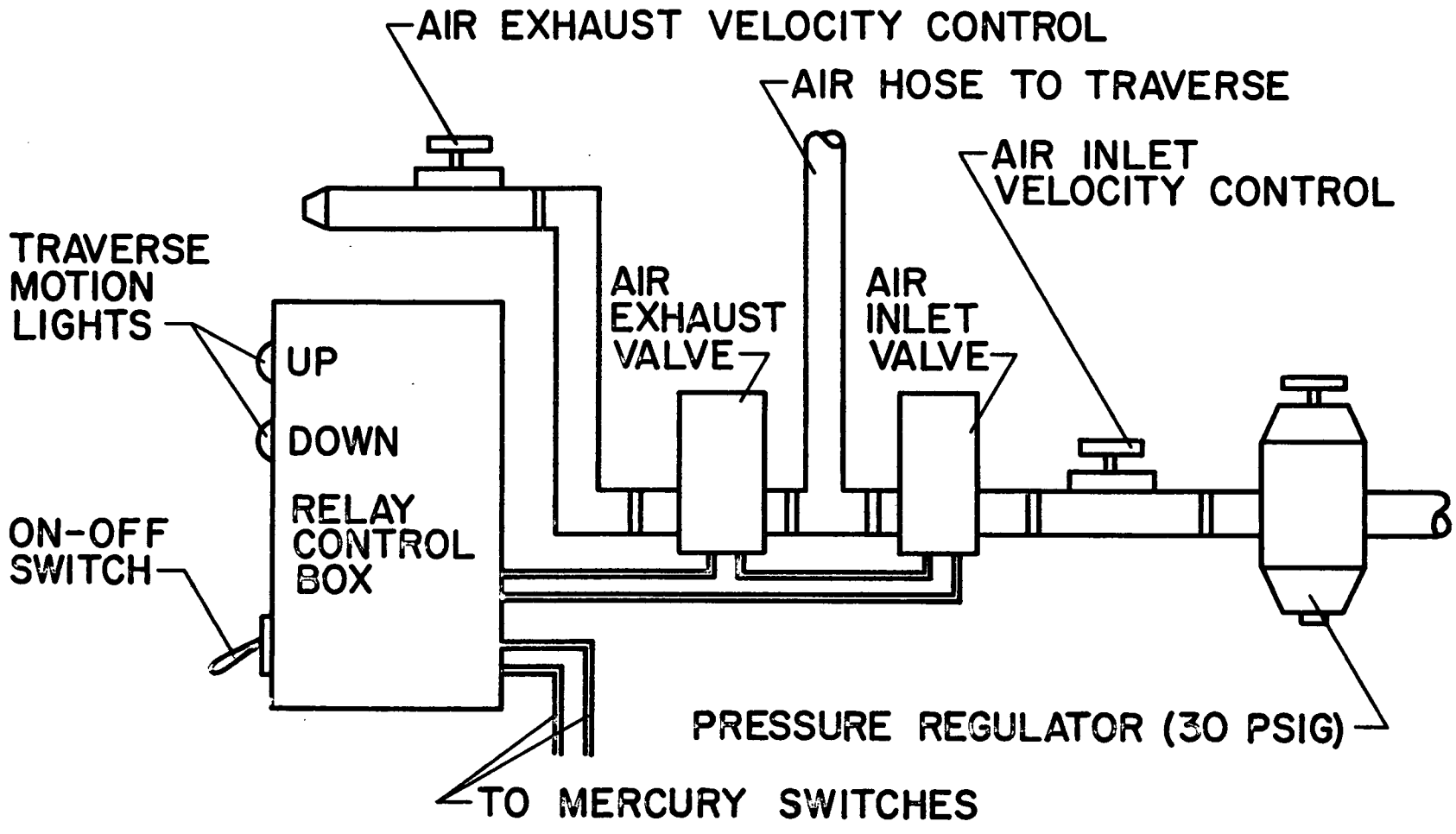

9.3 Simplified drawing of the control unit

The specifications of the traverse apparatus as it was finally constructed can now be determined utilizing Figure 9.4 which shows the traverse boom motion, greatly simplified. In list form, the specifications are:

Traverse arc angle $\cong 53°$,

Boom length $\cong$ 7 ft,

Traverse arc length $\cong$ 6.5 ft,

Boom velocity $\cong$ 20 traverses in 35 sec

= 1.75 sec/traverse,

Delay time for boom direction change $\cong$ 0.10 sec,

Time for one traverse = 1.75 - 0.10 = 1.65 sec,

Boom velocity = 6.5 ft/1.65 sec = 4 ft/sec.

In terms of a graphic recorder print-out with a paper speed of 30 mm/sec, this boom velocity corresponds to a traverse sweep length on paper of approximately 2.06 inches.

It should be understood that the above specifications are valid only when the traverse device is equipped with the seven foot boom utilized throughout this study. Should this boom length be increased or decreased, the specifications would change accordingly.

A photograph of the actual traverse device and its control unit are shown in Figure 9.5. As can be seen, both components of the total system are constructed of parts which are relatively inexpensive and easily obtained.

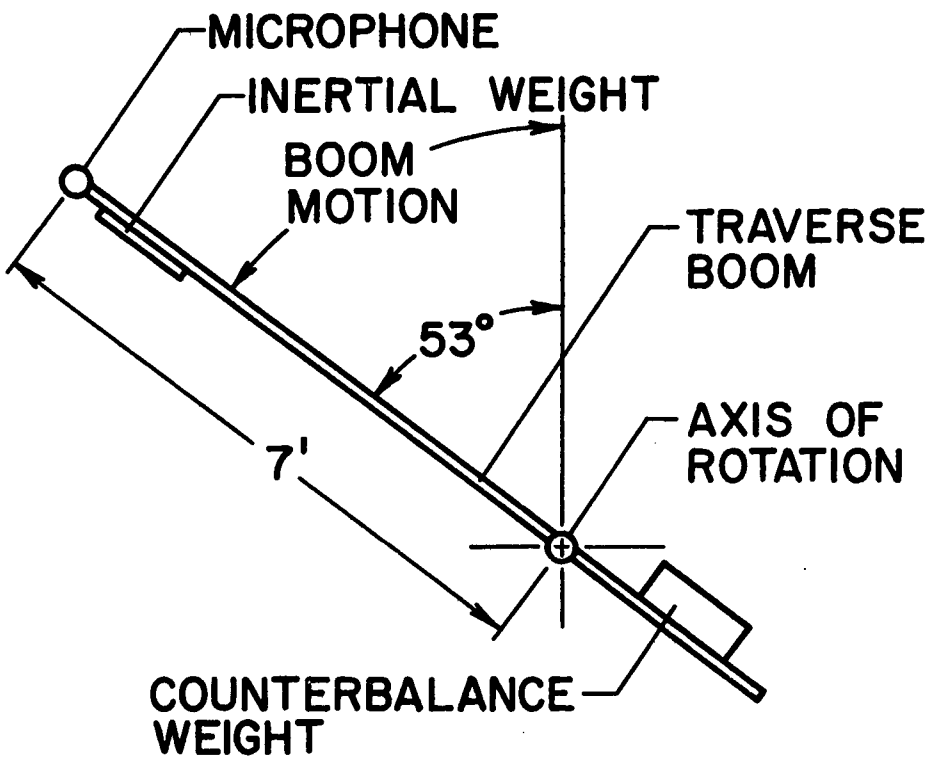

9.4 Simplified drawing of microphone boom motion

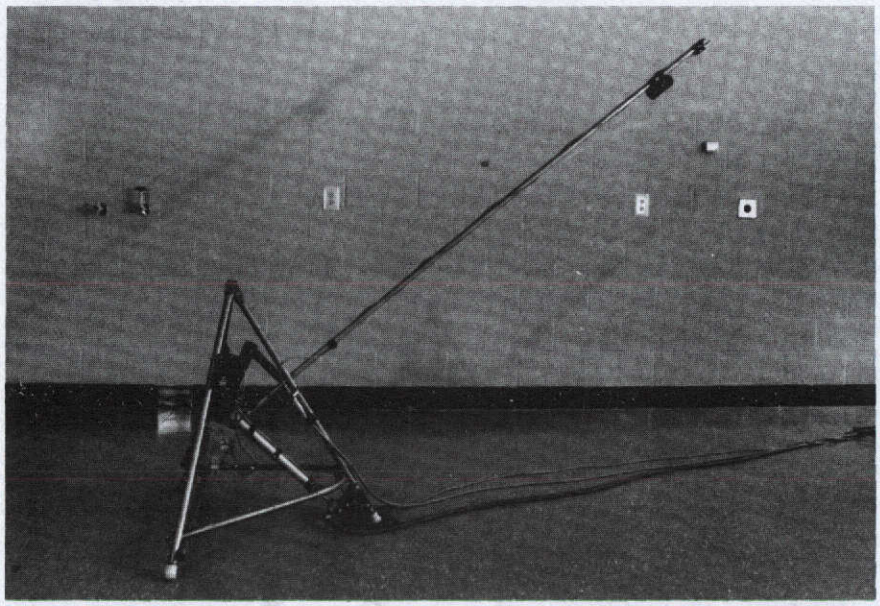

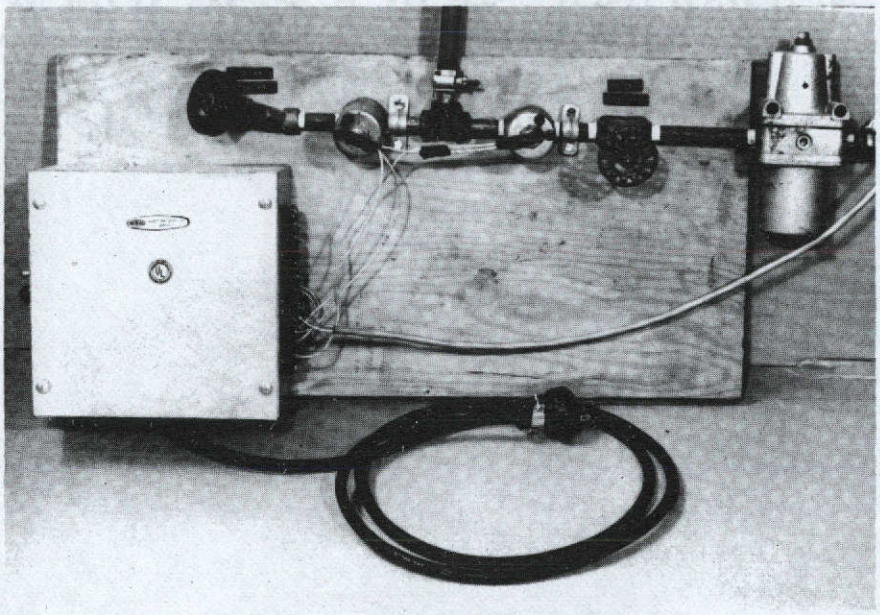

9.5 Photograph of microphone traverse mechanism and its control unit

9.3 Sample Calculation: Standard Deviation Within Source Positions

The procedure for calculating the standard deviation within source positions for a given data set was explained in detail in Chapter 5. Table 9.1 shows actual data taken for the 30 inch speaker at 250 Hz and at source position seven. Included in the table are the necessary mathematical calculations involved in the computation of the required standard deviation. The following symbols are used in the table.

SPL_i = sound pressure level at ith microphone location,

p/p_{Ri} = ratio of the actual acoustic pressure at microphone position i to the reference pressure of 0.0002 dy/cm,

$\overline{(p/p_R)^2}$ = spatial average squared sound pressure,

$\overline{SPL}$ = spatial average sound pressure level,

$\sigma_{dB}^2, \sigma_{dB}$ = variance and standard deviation in dB, respectively,

σ_A^2, σ_A = variance and standard deviation normalized to the mean square and the mean, respectively.

Having completed the computation shown in Table 9.1 for source position seven, the same procedure is utilized to analyze the remaining ten source positions. All eleven of the resulting uncertainties are then averaged to obtain the mean standard deviation within source positions for this data set. Table 9.2 shows the actual data, the calculated values, and the resulting mean standard deviation for the 30 inch speaker at 250 Hz.

Table 9.1 Sample calculation of the uncertainty of mean square pressure for a single microphone position using source position seven for the 30 inch speaker at 250 Hz

Microphone Position	SPL_i	$(SPL-\overline{SPL})_i^2$	$(p/p_R)_i^2$ x10^8	$[(p/p_R)^2-\overline{(p/p_R)^2}]_i^2$ x10^{16}
1	79	121.0	0.80	82.68
2	85	25.0	3.16	45.32
3	89	1.0	7.95	3.77
4	93	9.0	20.00	102.16
5	89	1.0	7.95	3.77
6	89	1.0	7.95	3.77
7	81	81.0	1.26	74.52
8	85	25.0	3.16	45.32
9	94	16.0	25.18	233.70
10	95	25.0	31.60	471.21
11	85	25.0	3.16	45.32
12	94	16.0	25.18	233.70
13	87	9.0	5.02	23.74
14	80	100.0	1.00	79.08
15	87	9.0	5.02	23.74

Table 9.1 (Continued)

$$\sum_{i=1}^{15} (p/p_R)_i^2 x10^8 \ /15 = 9.89x10^8 = \overline{(p/p_R)}^2 x10^8$$

$$10 \log \overline{(p/p_R)}^2 x10^8 = 89.97 \text{ dB} = \overline{SPL}$$

$$\sigma_{dB}^2 = \sum_{i=1}^{15} (SPL-\overline{SPL})_i^2 \ /14 = 33.14 \text{ dB}^2$$

$$\sigma dB = (\sigma_{dB}^2)^{1/2} = 5.75 \text{ dB}$$

$$\sigma_{AN}^2 = \sum_{i=1}^{15} [(p/p_R)^2 - \overline{(p/p_R)}^2]_i^2 \ x10^{16} \ /[14x\overline{(p/p_R)}^4 x10^{16}] = 1.07$$

$$\sigma_{AN} = (\sigma_{AN}^2)^{1/2} = 1.03$$

Table 9.2 Sample results for the average standard deviation of mean square pressure for a single microphone position using the 30 inch speaker at 250 Hz

Source Position	Standard Deviation (dB)	Standard Deviation (normal)
1	7.81	1.22
2	5.40	0.98
3	5.98	1.04
4	8.24	1.26
5	4.24	0.83
6	7.00	1.14
7	5.85	1.03
8	6.06	1.05
9	5.02	0.93
10	6.82	1.12
11	4.08	0.82
Average	6.04	1.04

9.4 Sample Calculation: Standard Deviation Among Source Positions

The procedure for calculating the standard deviation among source positions was given in detail in Chapter 5. Table 9.3 shows the spatial average sound pressure levels and the spatial average squared sound pressures which were calculated from data obtained for the 30 inch speaker at 250 Hz. Also included are the mathematical calculations which are necessary to yield the required standard deviations. The following symbols are used in the table.

$\overline{(p/p_R)^2}_j$ = spatial average squared pressure for the jth source position,

$\overline{SPL}_j$ = spatial average sound pressure level for source position j,

$\overline{\overline{(p/p_R)^2}}$ = mean value of the spatial average squared pressures,

$\overline{\overline{SPL}}$ = mean value of the spatial average sound pressure levels,

$\sigma_{dB}^2, \sigma_{dB}$ = variance and standard deviation in dB, respectively,

σ_A^2, σ_A = variance and standard deviation normalized to the square of the mean and the mean, respectively.

Table 9.3 Sample calculation of the uncertainty of sound power for a single source position using data taken for the 30 inch speaker at 250 Hz

Source Position	$\overline{SPL}_j$	$(\overline{SPL}-\overline{\overline{SPL}})_j^2$	$\overline{(p/p_R)^2}_j$	$[\overline{(p/p_R)^2}-\overline{\overline{(p/p_R)^2}}]^2$
1	86.75	4.750	4.74	9.550
2	88.78	0.020	7.55	0.078
3	88.05	0.770	6.41	2.016
4	88.06	0.176	6.42	1.988
5	89.35	0.176	8.63	0.640
6	89.42	0.240	8.75	0.846
7	89.97	1.080	9.89	4.243
8	88.89	0.002	7.75	0.006
9	89.80	0.757	9.57	3.028
10	88.20	0.532	6.61	1.488
11	89.92	0.980	9.83	4.000

$$\sum_{j=1}^{11} \overline{(p/p_R)^2}_j \times 10^8/11 = 7.83\times10^8 = \overline{\overline{(p/p_R)^2}} \times 10^8$$

$$10 \log \overline{\overline{(p/p_R)^2}} \times 10^8 = 88.93 \ \overline{\overline{SPL}}$$

$$\sigma_{dB}^2 = \sum_{j=1}^{11} (\overline{SPL}-\overline{\overline{SPL}})_j^2 /10 = 0.950 \ dB^2$$

Table 9.3 (Continued)

$$\sigma_{dB} = (\sigma^2_{dB})^{1/2} = 0.974 \text{ dB}$$

$$\sigma^2_{CN} = \sum_{j=1}^{11} [\overline{(p/p_R)^2} - \overline{(p/p_R)^2}]^2 x 10^{16} / [10 x \overline{(p/p_R)^4} x 10^{16}] = 0.045$$

$$\sigma_{CN} = (\sigma^2_{CN})^{1/2} = 0.213$$